การบำบัดน้ำเสียที่ปนเปื้อนด้วยยาปฏิชีวนะโดยใช้อนุภาคคาร์บอนระดับนาโนเมตรที่มีความเป็นแม่เหล็ก

นางสาวพลอยประไพ มงคลสมัย

วิทยานิพนธ์นี้เป็นส่วนหนึ่งของการศึกษาตามหลักสูตรปริญญาวิศวกรรมศาสตรมหาบัณฑิต
สาขาวิชาวิศวกรรมเคมี ภาควิชาวิศวกรรมเคมี
คณะวิศวกรรมศาสตร์ จุฬาลงกรณ์มหาวิทยาลัย
ปีการศึกษา 2556

TREATMENT OF WASTEWATER CONTAMINATED WITH ANTIBIOTICS
USING MAGNETIC CARBON NANOPARTICLES

Miss Ployprapai Mongkolsamai

A Thesis Submitted in Partial Fulfillment of the Requirements
for the Degree of Master of Engineering Program in Chemical Engineering
Department of Chemical Engineering
Faculty of Engineering
Chulalongkorn University
Academic Year 2013
Copyright of Chulalongkorn University

Thesis Title   TREATMENT OF WASTEWATER CONTAMINATED WITH ANTIBIOTICS USING MAGNETIC CARBON NANOPARTICLES

By   Miss Ployprapai Mongkolsamai

Field of Study   Chemical Engineering

Thesis Advisor   Associate Professor Tawatchai Charinpanitkul, D.Eng.

    Accepted by the Faculty of Engineering, Chulalongkorn University in Partial Fulfillment of the Requirements for the Master's Degree

    ....Dean of the Faculty of Engineering

    (Professor Bundhit Eua-Arporn, Ph.D.)

THESIS COMMITTEE

    ....Chairman

    (Associate Professor Bunjerd Jongsomjit, Ph.D.)

    ....Thesis Advisor

    (Associate Professor Tawatchai Charinpanitkul, D.Eng.)

    ....Examiner

    (Assistant Professor Apinan Soottitantawat, D.Eng.)

    ....External Examiner

    (Kajornsak Faungnawakij, D.Eng.)

พลอยประไพ มงคลสมัย : การบำบัดน้ำเสียที่ปนเปื้อนด้วยยาปฏิชีวนะ โดยใช้อนุภาคคาร์บอนระดับ
นาโนเมตรที่มีความเป็นแม่เหล็ก (TREATMENT OF WASTEWATER CONTAMINATED WITH
ANTIBIOTICS USING MAGNETIC CARBON NANOPARTICLES) อ. ที่ปรึกษาวิทยานิพนธ์
หลัก: รศ.ดร. ธวัชชัย ชรินพาณิชกุล, 88 หน้า

     ในงานวิจัยนี้ได้ศึกษาเกี่ยวกับการสังเคราะห์อนุภาคคาร์บอนระดับนาโนเมตรที่มีความเป็นแม่เหล็ก
ด้วยวิธีการไพโรไลซิสร่วมระหว่างเอทานอลและเฟอร์โรซีนซึ่งจัดเป็นแหล่งคาร์บอนและตัวเร่งปฏิกิริยา
ตามลำดับ โดยทำการศึกษาอิทธิพลของอุณหภูมิในการไพโรไลซิ   สในช่วง 700-900 องศาเซลเซียส และ
อัตราส่วนของเฟอร์โรซีนต่อเอทานอลระหว่างร้อยละ5-9 โดยน้ำหนัก ทั้งนี้เพื่อศึกษาหาสภาวะที่เหมาะสมใน
การสังเคราะห์อนุภาคคาร์บอนระดับนาโนเมตรที่มีความเป็นแม่เหล็กเพื่อนำไปประยุกต์ใช้เป็นตัวดูดซับยา
ปฏิชีวนะ ประเภทเตตร้าไซคลินได้อย่ างมีประสิทธิภาพที่สุด โดยคุณสมบัติความเป็นแม่เหล็กของอนุภาคที่
สังเคราะห์ได้นั้นจะเป็นประโยชน์ในการแยกอนุภาคที่ใช้เป็นตัวดูดซับออกจากสารละลายยาปฏิชีวนะเตตร้า
ไซคลินโดยใช้แม่เหล็กถาวร

     จากการทดลองพบว่าอนุภาคคาร์บอนระดับนาโนเมตรที่สังเคราะห์ที่อุณหภูมิ   700 องศาเซลเซียส
และอัตราส่วนระหว่างเฟอร์โรซีนต่อเอทานอลเป็น   ร้อยละ 9 โดยน้ำหนัก ให้ค่าพื้นที่ผิวจำเพาะที่สูงที่สุดคือ
47.12 มิลลิกรัมต่อกรัม และมีขนาดเส้นผ่านศูนย์กลางรูพรุนคือ 14.46 นาโนเมตร ซึ่งจัดเป็นรูพรุนขนาดกลาง
ทั้งนี้อนุภาคที่สังเคราะห์ที่สภาวะนี้ยังให้ประสิทธิภาพในการดูดซับยาปฏิชีวนะสูงกว่าที่สภาวะอื่นๆด้วย เมื่อ
ศึกษาถึงลักษณะทางสัณฐานวิทยาของอนุภาคที่สังเคราะห์ได้พบว่ามีลักษณะเป็นท่อคาร์บอนระดับนาโนเมตร
และ แคปซูลคาร์บอนระดับนาโนเมตร โดยมีอนุภาคของเหล็กที่ใช้เป็นตัวเร่งปฏิกิริยาบรรจุภายในอนุภาค
เหล่านี้

     ในการประยุกต์ใช้อนุภาคคาร์บอนระดับนาโนเมตรเป็นตัวดูดซับยาปฏิชีวนะเตตร้าไซคลินนั้นพบว่า
ปริมาณของอนุภาคที่ใช้ในการดูดซับที่เหมาะสมที่สุดคือ 8 มิลลิกรัมต่อสารละลาย 25 มิลลิลิตรและค่า ความ
เป็นกรดด่างคือ 5 ทั้งนี้พบว่าเมื่ออุณหภูมิสูงขึ้นอนุภาคคาร์บอนระดับนาโนเมตรจะ สามารถดูดซับยาปฏิชีวนะ
ได้สูงขึ้นด้วย โดยระบบจะเข้าสู่สมดุลภายใน 180 นาที จากผลการทดลองพบว่าการดูดซับยาปฏิชีวนะเตตร้า
ไซคลินสามารถอธิบายได้ด้วยแบบจำลองทางคณิตศาสตร์จลนพลศาสตร์การดูดซับอันดับสองเทียมและสมดุล
ของการดูดซับเป็นไปตามแบบจำลองสมดุลสมการของฟรุนดริช

ภาควิชา   วิศวกรรมเคมี   ลายมือชื่อนิสิต
สาขาวิชา   วิศวกรรมเคมี   ลายมือชื่อ อ.ที่ปรึกษาวิทยานิพนธ์หลัก
ปีการศึกษา   2556

5470295021: MAJOR   CHEMICAL ENGINEERING
KEYWORDS :   CARBON NANOPARTICLES / PYROLYSIS / MAGNETIC / ADSORPTION / ANTIBIOTICS / TETRACYCLINE

PLOYPRAPAI MONGKOLSAMAI: TREATMENT OF WASTEWATER CONTAMINATED WITH ANTIBIOTICS USING MAGNETIC CARBON NANOPARTICLES.   ADVISOR: ASSOC.   PROF.   TAWATCHAI CHARINPANITKUL, D.Eng., 88 pp.

Magnetic carbon nanoparticle (M-CNPs) was synthesized by using ethanol and ferrocene. The parameter that studied consist of the synthesizing temperature between 700-900°C and the ratio of ferrocene to ethanol was in the range of 5-9wt% to find the appropriate condition for use as an adsorbent for adsorption tetracycline. Such M-CNPs would be beneficial for their collection using a permanent magnet.

From the results, the synthesizing temperature was 700°C and the ratio of ferrocene to ethanol was 9wt% showed the highest specific surface area about 47.12 m^2/g and pore diameter of 14.46 nm that could be indicated as mesopore. However, the adsorption efficiency of the synthesized M-CNPs in the condition showed higher than the other condition. The synthesized M-CNPs consist of two distinctively different nanostructures, namely multi-walled carbon nanotubes and carbon nanocapsules with iron nanoparticles attached inside these particles.

Application of synthesized M-CNPs as an adsorbent for tetracycline indicated 8 mg per 25 mL of solution was the optimal amount of M-CNPs loading and the pH value was 5. When increasing temperature will result to adsorption capacity increase from 24.04, 58.93 to 82.81 mg/g when temperature increased from 25, 45 to 65°C. For the effect of contact time, the adsorption would reach equilibrium within 180 min. The kinetic model was better fitted by pseudo-second-order and Freundlich model for adsorption isotherm.

Department : ....Chemical Engineering....   Student's Signature ....
Field of Study : ..Chemical Engineering....   Advisor's Signature ....
Academic Year : ..2013............................

ACKNOWLEDGEMENTS

CONTENTS

LIST OF TABLES

LIST OF FIGURES

CHAPTER I

INTRODUCTION

1.1   Background and Motivation

Antibiotics are drugs that stop or slow down the growth of bacteria which would be necessary for enhancing the growth of animals. They are commonly used in many fields, such as agriculture, medicine and industry, etc.   Because of their complex structures, they are difficult to decompose naturally. Therefore once they are released to the surrounding, they would contaminate some water resources.   In general, wastewater treatment plants would not specifically be designed for such antibiotic therapy. It has been reported that many water resources have been increasingly contaminated with antibiotics.   Without sufficient treatment, contamination of antibiotics in the environment would result in the destruction of useful bacteria. There are many reports that most antibiotics cannot be absorbed and digested well. Leakage of antibiotics released from human-made activities will enter into the surface water, inducing an increase in microbial resistance, which affects the ecosystem [1, 2].   However, the problem of accumulated antibiotics in the environment is major problem that could affect the well-being of living organisms should be studied and resolved quickly.

The adsorption technology is gaining attention for treatment of wastewater contaminated with heavy metals and organic compounds due to its simplicity of design, efficiency, low cost and wide adaptability[3]. At presence, commonly used adsorbents would be activated carbons, clays and zeolites [4].   However, those adsorbents have low adsorption capacities and difficult to separate from the solution after adsorption [5].   Therefore, it is increasing requirement to study new promising adsorbent technology.

Carbon nanoparticles (CNPs) with magnetic properties have attracted and increasing interest, due to their unique electronic and magnetic properties [6] with the suitable features such as large specific surface area, hollow and layered structures

made of CNPs were used as an adsorbent for removing environmental pollutants (e.g. heavy metal ions, small molecules, and organic chemicals) [7, 8]. The outstanding feature of the magnetic made that CNPs can be separated from the solution by using a simple magnetic process [9] which can be separated easily, quickly, and save energy for the centrifugation. Compared with other types of adsorbents such as activated carbon, it was reported shown that CNPs can be more effective than activated carbon because of their higher adsorption capacities for heavy metals, phenols, and other organic chemicals and shorter equilibrium times [10, 11]. There are many methods for CNPs synthesis such as arc discharge, laser ablation, and chemical vapor deposition (CVD). Co-pyrolysis is a type of CVD method that can produce CNPs at low in large quantity [12] and has the advantage of permitting the use of solid, liquid and gaseous carbon precursors [13].

Due to the current energy shortage. The Thai government has been encouraging the production of ethanol from agricultural products to be blended with gasoline for the purpose is to reduce imports of foreign oil, but ethanol is used to produce gasohol must have very high purity. However, the production of ethanol from agricultural products that have contaminated quite a lot. Purification requires high energy and increase the cost. So finding a new alternative for ethanol with a low purity will be the key.

In this work, the importance of a specific issue including magnetic carbon nanoparticles (M-CNPs) to be synthesized from ethanol as the carbon source and ferrocene as a catalyst through the co-pyrolysis will be applied as an adsorbent for removal of antibiotic contaminating in simulated wastewater. It should be noted that magnetic properties is a unique characteristic which is essential for a separation process using a simple magnetic process. Study of optimized conditions of M-CNP synthesis and adsorption conditions for removal of antibiotics will be investigated and discussed.

1.2   Objectives of the research

The main objective of this research is to synthesize magnetic carbon nanoparticles (M-CNPs) by co-pyrolysis of ethanol and ferrocene as carbon source

and catalyst, respectively. Also, adsorption of Tetracycline as a typical antibiotic from simulated wastewater onto the synthesized M-CNPs will be experimentally investigated and discussed.

1.3   Scope of the research

The scope of this research is set to focus on experimental investigation in laboratory-scale system, which includes the following issues.

1.3.1   Synthesis of magnetic carbon nanoparticles (M-CNPs) by co-pyrolysis of ethanol and ferrocene.

1.3.1.1 Ferrocene to ethanol ratio is varied in the range of
7 wt% - 9 wt%.

1.3.1.2 Synthesizing temperature is varied from 700-900°C.

1.3.1.3 Carrier gas (nitrogen gas) flow rate is 2 L/min.

1.3.1.4 Characterization of synthesized M-CNPs morphology   and properties will   be conducted by

- Scanning Electron Microscopy (SEM) and Transmission Electron   Microscope (TEM) for synthesized M-CNPs morphology.

- X-ray diffraction (XRD) for structure and chemical composition of synthesized M-CNPs.

- Zetasizer for surface charge properties of synthesized M-CNPs.

- BET for determine of the surface area and pore structure of synthesized M-CNPs.

- Raman spectroscopy for crystallinity of synthesized M-CNPs.

     1.3.2   Adsorption of antibiotics from wastewater by using the synthesized M-CNPs as:

     1.3.2.1 Dispersion of typical antibiotics (Tetracycline) in de-ionized water and effect of adsorption will be studied as follow:
- Study effect of amount of M-CNPs loading.
- Study effect of initial pH
- Study effect of temperature (adsorption kinetics and adsorption isotherm)

     1.3.2.2 Characterization of adsorbed antibiotics on M-CNPs will be conducted by
- UV-VIS Spectrophotometer for measured the concentration of antibiotics in wastewater after adsorption.

1.4   Procedures of the research

1.4.1   Review and survey related literatures.

1.4.2   Set up experiment and equipment (chemicals and apparatus).

1.4.3   Synthesis of M-CNPs by co-pyrolysis of ethanol and ferrocene.

1.4.4   Examine optimized conditions for synthesis of M-CNPs.

1.4.5   Carry out experiments by various conditions of adsorption antibiotics on M-CNPs.

1.4.6   Discuss and conclude experimental results.

1.4.7   Summarize all experimental findings to write thesis and technical paper.

1.5   Expected benefits

Expected benefits from this investigated will be the knowledge in synthesis of M-CNPs by co-pyrolysis of ethanol and ferrocene and the adsorption of antibiotics from wastewater by using synthesized M-CNPs.

CHAPTER II

THEORY AND LITERATURE REVIEW

2.1 Carbon Nanoparticles (CNPs)

Carbon is the main element in living organisms. There are many carbon allotropes such as amorphous carbon, graphite, diamond and buckminsterfullerene. Carbon nanoparticles are considered as composed structures with the nanometer size. The chronicle of carbon nanoparticles (CNPs) started in 1985, the Buckminsterfullerene (C_{60}) was discovered by Kroto [14]. After that, the amount of discovered CNPs is rapidly increasing such as carbon nanotubes (CNTs), carbon nanohorns (CNHs), carbon nanocapsules (CNCs) and so on.

2.1.1 Buckminsterfullerene (C_{60})

Buckminsterfullerene (C_{60}) as shown in Figure 2.1 is a substance with spherical molecular structure contains 60 carbon atoms. The diameter of a C_{60} molecule is about 1.01 nm and the structure of C_{60} consists of 20 hexagons and 12 pentagons. C_{60} is the organic molecules that have the most symmetrical shape, thereafter carbon with a larger molecule size than the C_{60} such as C_{70}, C_{240} and C_{540} was discovered at a later time. Buckminsterfullerene is a structure with high symmetry. It is a structure that is very strong as well. Nowadays, the Buckminsterfullerene is used in nanoelectronics because their semiconductor properties including applied in the medical and many other industries.
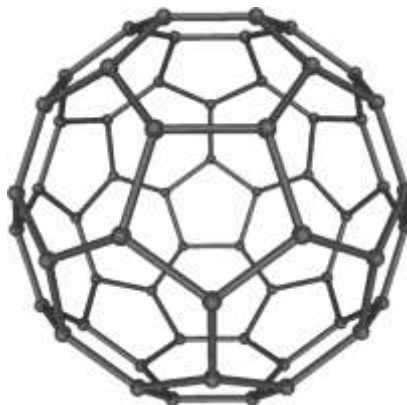
Figure 2.1 Structures of Buckminsterfullerene (C_{60})

(http://inventorspot.com/articles/bucky_balls_32825)

2.1.2 Carbon nanotubes (CNTs)

Carbon nanotubes (CNTs), a type of fullerene as shown in Figure 2.2 have been discovered by Ijima in 1991 [15] which can be described as graphene sheet rolled into a cylindrical shape with both open or closed ends. The chemical bonding of CNTs are composed entirely of sp^2 C-C bonds. CNTs can be divided into two types that are single-walled carbon nanotubes (SWCNTs) and multi-walled carbon nanotubes (MWCNTs). SWCNTs are tubes of graphene that have a single cylindrical wall. The structure of SWCNTs can be conceptualized as a layer of graphene roll up to cylindrical with a few nanometers of diameter and several centimeters of length. MWCNTs are tubes which have multi cylindrical wall with a diameter of 10 to 300 nm, and the distance between the walls is 0.34 to 0.36 nm.

Carbon nanotubes formed by the rolling of a sheet of graphene. So if the direction to roll is different, it also makes carbon nanotubes have different properties. The rolling type of graphene to form CNTs can be divided into 3 types consist of armchair, zig-zag, and chiral as depict in Figure 2.3. For armchair carbon nanotubes, it has electrical properties related to metals and is a better conductor than copper or any other metal. The zigzag and chiral carbon nanotubes have electrical properties similar to semiconductors.

CNTs have attracted considerable interest due to their unique structural, physical and chemical properties and thus their potential for use in many applications such as electronics, optics, nanotechnology, industrial, architecture and materials science.

(a)   (b)
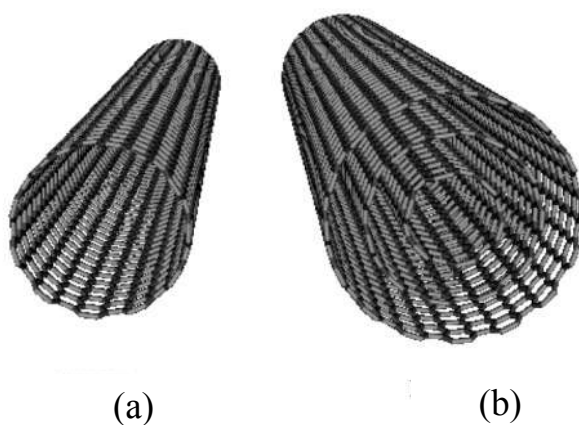
Figure 2.2 Structures of (a) SWCNTs and (b) MWCNTs

(http://www-ibmc.u-strasbg.fr)

armchair   zigzag   chiral
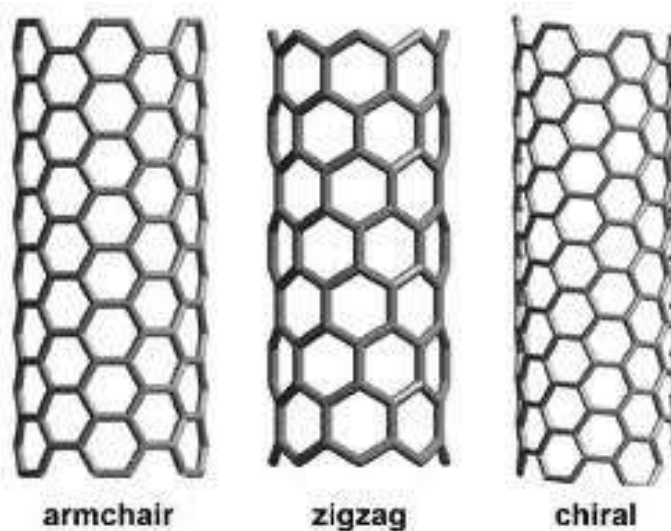
Figure 2.3 Configurations of carbon nanotubes

(http://www.teachers.yale.edu)

2.1.3 Carbon nanohorns (CNHs)

Carbon nanohorns (CNHs) were discovered by Iijima's research group in 1999. Their irregular shape like horn with the diameter of 2-5 nm, the length of 40-50 nm and cone angle of approximately 20°. Generally, thousands of SWCNHs assemble to form the ‚dahlia-like' and ‚bud-like' structured aggregates with the diameters about 100 nm (see Figure 2.4). Their unique structures such as high surface area and microporosity lead SWNHs become a promising material for drug delivery, gas adsorption, and electrode for a fuel cell.
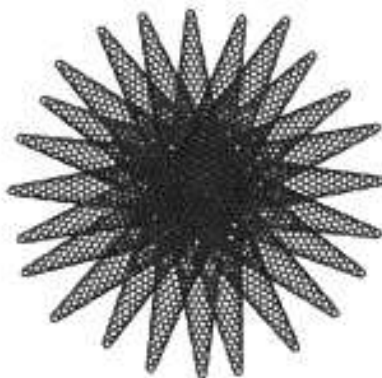
Figure 2.4 Structures of CNHs
(http://www-ibmc.u-strasbg.fr)

2.1.4 Carbon nanocapsules (CNCs)

And a novel sphere-like carbon nanocapsules (CNCs), it is a particle that contain with metals encapsulated (such as Fe, Co and Ni) by grapheme layer as shown in Figure 2.5 the carbon-coated magnetic nanoparticles might have many potential applications such as magnetic data storage devices, magnetic force microscopy and biomedicines according to the magnetic properties of the metal that be wrapped.

Figure 2.5 Structures of CNCs

(http://www.den.hokudai.ac.jp)

2.2   Synthesis of carbon nanoparticles

Recently, there are some methods such as laser ablation, arc discharge and chemical vapor deposition (CVD) have been investigated for synthesis carbon nanoparticles. For details of this method would be shown below.

2.2.1   Laser ablation method

This method was discovered by Small et al. (1995) [16] while they were investigating about the effect of laser strike on metals. At first, a pulsed laser as an energy source is struck to the carbon target with catalytic metal (such as Ni, Co, Pt and Cu) at high temperature in the presence of inert gas such as helium that vaporizes a carbon target after the temperature cool down the carbon nanotubes would form as soot on the surfaces of the reactor, as the vaporized carbon condenses. This method can produced the single walled carbon nanotubes with high yield (>70%) by using graphite rods with Ni and Co at 1200°C. The carbon nanotubes that generated in this method would have diameter of 10-20 nm with the length up to 10 micron or more. However, various condition such as temperature, carbon source and catalyst composition would be effected to the generated carbon nanotubes[17]. A picture for laser ablation method is shown in Figure 2.6.
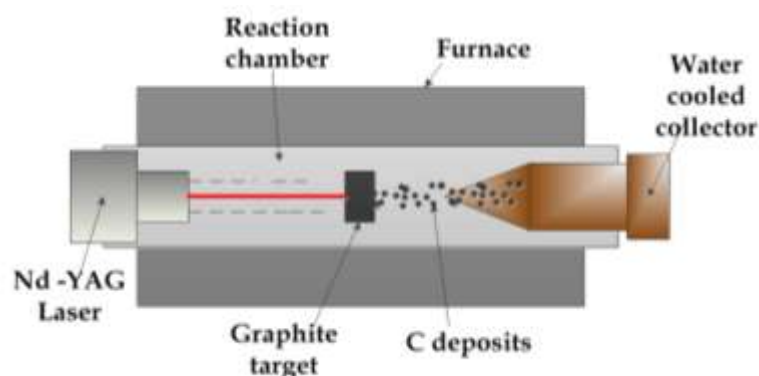
Figure 2.6 Laser ablation method

(www.intechopen.com)

2.2.2   Arc discharge method

Arc discharge method, first utilized by Iijima (1991) [15], use electric current as an energy source that can occur both in water and liquid nitrogen. The two electrodes by using graphite rods act an anode and the bigger one as a cathode, respectively. These electrodes were installed at the center of chamber. However, there is an iron in a superficial dip at the cathode as shown as the catalyst metal. The arc would be happened by running of DC current about 200A at 20V between the electrodes at high temperature after that the carbon source would vaporize and generate the plasma zone. Afterwards the vaporized carbon at the plasma zone would be re-condensed into the soot when temperature is cooled down. The carbon nanoparticles would be generated on the iron catalyst in cathode that has diameter ranging from 4-30 nm and length up to 1 mm. The schematic of arc discharge method is shown in Figure2.7.
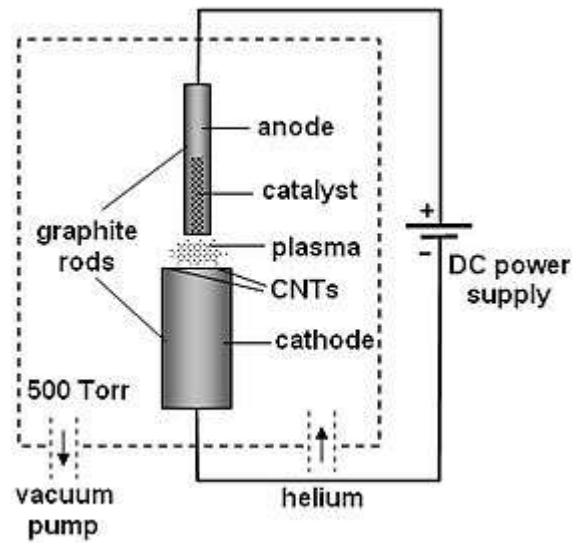
Figure 2.7 Arc discharge method

(http://th.wikipedia.org/wiki)

2.2.3   Chemical Vapor Deposition, CVD

Chemical vapor deposition method as show in Figure 2.8 have started utilizing in 1996, this method used the thermal from coil as an energy source. It begin with the catalytic metal such as Fe, Ni and Co would be deposited on substrates (Silicon, glass and alumina) and placed into the quartz tube with be heated to temperature about 700-900°C to generation the catalyst metals nanoparticles. The hydrocarbon gas (methane, ethylene or acetylene) which acted as a carbon source will lead into the quartz tube by carried gas such as argon, nitrogen and helium. After that the hydrocarbon will decompose into carbon cluster and diffuse and grow on catalyst metal (substrate). The catalyst metal can stay both top and bottom in carbon nanoparticles. CVD method can produce the large scale production of carbon nanoparticles. However, this method can be divided into many type such as thermal chemical vapor deposition, plasma enhanced chemical vapor deposition, vapor phase growth and co-pyrolysis.

For co-pyrolysis is the one type of CVD. The advantages of co-pyrolysis are unnecessary to use substrates and can use the carbon source which is solid, liquid and gas. This method mostly used ferrocene as a catalytic metal and the solid carbon

source such as glycerol and naphthalene. The precursor will load in the ceramic boat and place into the front of quartz tube when temperature is heated to the design temperature (about 700-1000°C) the carrier gas will lead the vapor of the mixture precursor to the middle of the quartz tube that have high enough temperature to form carbon nanoparticles. The carbon nanoparticles will deposit in the inner wall of quartz tube.
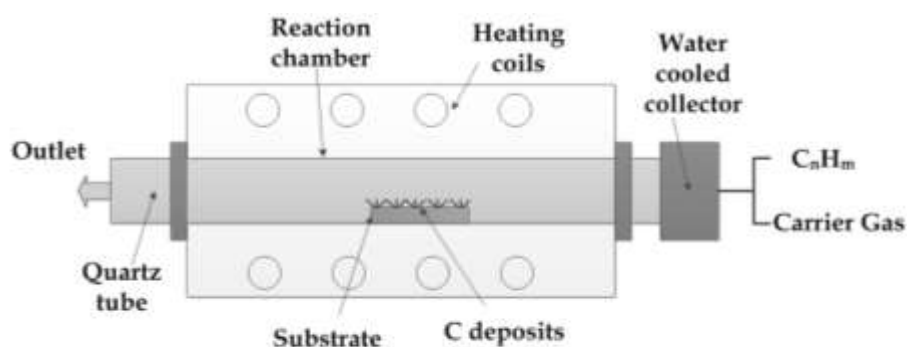
Figure 2.8 Chemical vapor deposition

(www.intechopen.com**)**

2.3   Antibiotics

In 1942, antibiotics were coined by Selman Waksman to explain any drug or substance that stop or slow down the growth of bacteria. They are derived from some microorganisms such as bacteria, fungi or microbes. At present, antibiotics are used to resist infection from outside the body or some object and some species are used to accelerate the growth in animals. Thus, antibiotics are commonly used in many fields such as agriculture, medicine and industry, etc. Antibiotics can be divided into two categories according to the origin that are drug which contains chemicals that come from living organisms and synthetic antibiotics. In addition to that antibiotics can be classified based on their mechanism of action, chemical structure, or spectrum of activity. There are many target of antibiotics on bacterial such as the bacterial cell

wall (penicillins, cephalosporins and monobactams), the cell membrane (polymixins, daptomycin and gramicidins), obstruct with essential bacterial enzymes (quinolones and sulfonamides) and protein synthesis (tetracyclines, macrolides and aminoglycosides). These antibiotics are used for different applications such as chloramphenical and oxytetracycline was used in agriculture, vancomycin and streptomycin were used in hospitals and in community use of Tetracycline, etc.

The most antibiotic cannot digested and adsorbed well in being then it released with excrement and urine to the environment and contaminated in ground, water, sediments and soils [2, 18] that effected to the ecology by increasing the resistance of microorganism.

Tetracycline

Tetracycline (TC) is part of tetracyclines (TCs) that a large family of antibiotics that is discovered by Benjamin Minge Duggar in 1945 and first designated in 1948. At first chlortetracycline and oxytetracycline are produced by *Streptomyces aureofaciens* and *Streptomyces rimosus,* respectively, and followed by other derivatives such as tetracycline, demethylchlortetracycline and others, including semi-synthetic derivatives[18]. For tetracycline and chlortetracycline is the product of *Streptomyces aureofaciens*.

Tetracyclines are the first broad-spectrum antibiotics [19] that effective to against many bacterial infections asuch as against many gram-positive, gram-negative bacteria, rickettsia and including the conjunctivitis agent. It is an inhibitor of protein synthesis by blocking the charged of aminoacyl-tRNA to the site on the ribosome. The structure of tetracyclines composes with a tetracyclic naphtacene carboxamide ring, the derivatives of tetracyclines would be differences the substitutions at position 5, 6 and 7. The structure of tetracycline and their derivatives such as oxytetracycline, chlortetracycline and demethylchlortetracycline is shown in Figure 2.9.
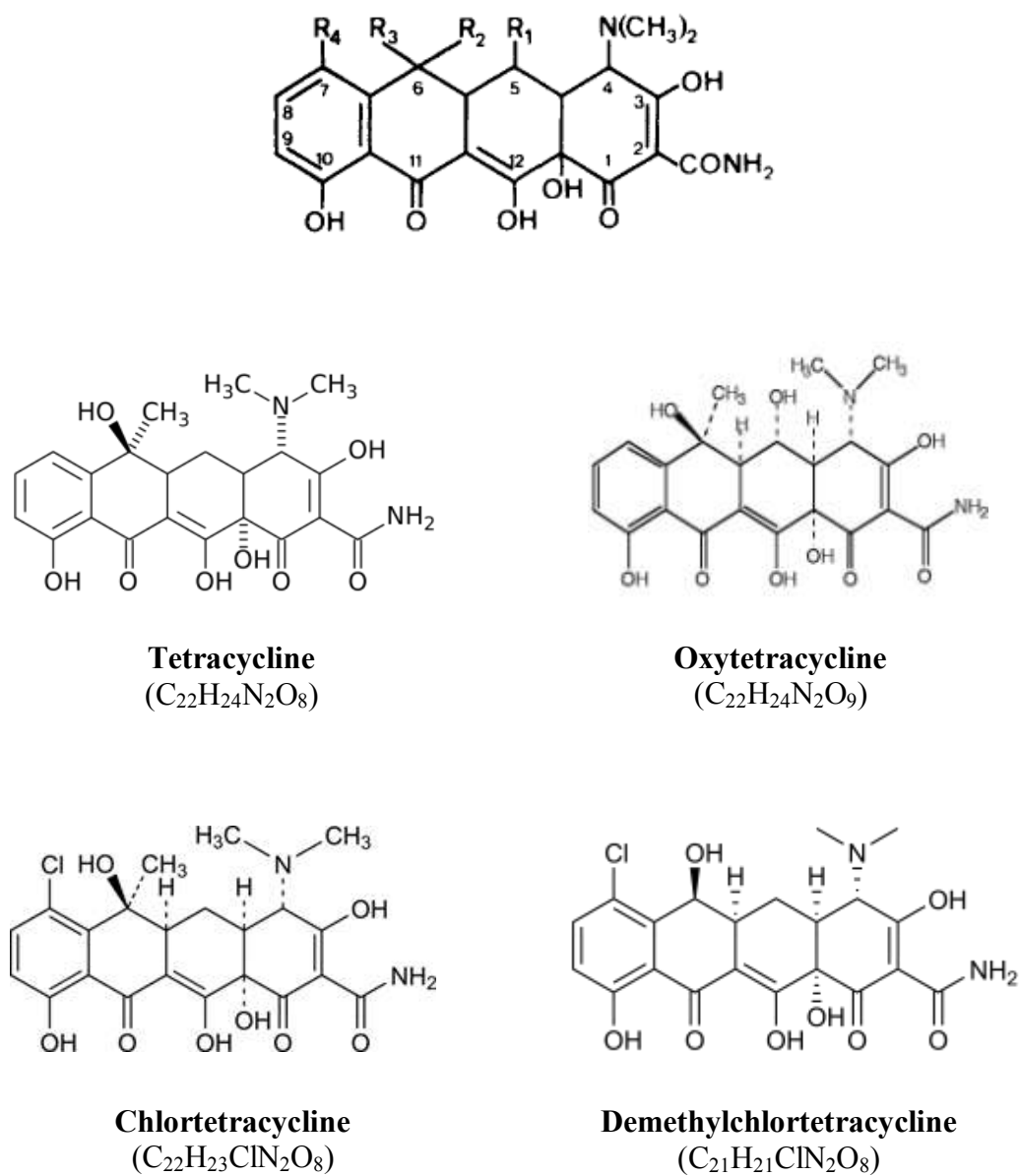
Figure 2.9 Structure of tetracyclines derivatives playing the differences of substitutions at position 5, 6 and 7[19]

2.4 Adsorption process

Adsorption is separation process, a substance that is extracted is called adsorbate which are dissolved in the fluid (liquid or gas). The fluid will flow into contact with the solid, which is called adsorbent, the adsorbate particles are diffused onto the surface of the adsorbent through the interface between solid and liquid. Therefore, to achieve high absorption, the adsorbent material should be have highly porous and connected with other pore to give high surface area.

The mechanism of adsorption is divided into 3 stages. First, external diffusion is the molecules of the adsorbate in fluid moves to the outer surface of the adsorbent and then the molecules of the adsorbate will diffuse into the pore of adsorbent, this step is called intraparticle diffusion or pore diffusion. Finally, adsorption step is the adhesion on porous surfaces between adsorbate and the surface of adsorbent.

Adsorption process can be divided into two types based on the intermolecular forces between the molecules of adsorbate with the surface of the adsorbent, if it showed van der waal's force that can be indicated the physical adsorption and chemical adsorption if have the formation of chemical bond between adsorbate and adsorbent.

2.4.1 Physical adsorption

For physical adsorption, it is a reversible process due to the operation of weak forces of attraction or Van der Waal's force (that consist of London dispersion force and Electrostatic force) between molecules. The adsorption with the weak force make physical adsorption has exothermic less than 20 kJ/mol then it can be easily reversed by heating or by decreasing the pressure which is the advantage for regeneration of adsorbent. Physical adsorption, adsorbate will capture and hold on adsorbent in multilayer. At first, the physical adsorption begins as a monolayer and then become to multilayer. The adsorption takes place until the pores are filled with adsorbate. However, the maximum capacity of adsorbent is related to the pore volume than to the surface area.

2.4.2 Chemical adsorption

For chemical adsorption, the formation of chemical bond between the adsorbate and adsorbent is strong force (ionic or covalent bonds) which involves the transfer of electrons between atoms. In this adsorption the bond between the atom will be destroyed and then rearrange the new bond with chemical bonds and the activation energy would be involved. The heat of chemical adsorption is in the range of 40-400 kJ/mol which often with a release of heat more than the heat of condensation that made the process is seldom reversible and the adhesion of the adsorbate on the surface of the adsorbent is monolayer. Table 2.1 is shown the details of the physical adsorption compare with the chemical adsorption.

Table 2.1 The comparison between physical adsorption and chemical adsorption

Types	Physical adsorption	Chemical adsorption
1. Heat of adsorption	in the range of 20-40 kJ/mol	in the range of 40-400 kJ/mol
2. Force of attraction	Van der Waal's forces	Chemical bond forces (ionic or covalent bonds)
3. The effect of temperature	takes place at low temperature	takes place at high temperature
4. The reversible adsorption process	reversible	irreversible
5. Specificity between adsorbate and adsorbent	not very specific	highly specific
6. The layers of adsorption	multilayers	monolayers

2.5   Adsorption isotherm

Adsorption isotherm is a relation between the amount of an adsorbate that is adsorbed on the surface of adsorbent with the concentration of solution at equilibrium and constant temperature. It is useful in the investigation of the adsorption of contaminants in water, to compare the best type of adsorbent. Adsorption Isotherm has many types to explain the equilibrium of adsorption. The most famous adsorption isotherm consists of the Langmuir and Freundlich isotherm, the details of two type of adsorption isotherm would be shown below.

2.5.1   Langmuir isotherm

In 1916, Irving Langmuir [20] offered the adsorption isotherm that depends on the balance between condensation and evaporation of adsorbed molecule. This isotherm can be applied for monolayer adsorption and physical adsorption that involved with the following assumptions.

- The surface of the adsorbent is uniform, that all the adsorption sites are equal.
- Adsorbed molecules do not interact.
- All adsorption take place through the same mechanism.
- Only a monolayer is formed at the maximum adsorption.

The Langmuir isotherm is the theoretical that agreeable for adsorption of a solute from a liquid solution as monolayer adsorption on a surface containing a finite number of approval sites. The Langmuir isotherm assumes uniform energies of adsorption onto the surface of adsorbent without transmigration of adsorbate in the plane of the surface. The Langmuir equation is shown in Equation 2.1 and 2.2.

Langmuir equation:
$$\frac{C_e}{Q_e} = \frac{C_e}{Q_m} + \frac{1}{K_L Q_m}$$
(2.1)

and
$$R_L = \frac{1}{1 + K_L C_0}$$
(2.2)

where

C_e (mg/L)	=	the concentration of adsorbate at equilibrium
Q_e (mg/g)	=	the amount of adsorbate adsorbed at equilibrium
Q_m (mg/g)	=	the maximum adsorption capacity
K_L (L/mg)	=	the Langmuir adsorption equilibrium constant

For the values of Q_m and K_L can be calculates from plotting C_e/Q_e versus C_e. The value of RL can be defined as below:

$R_L=0$	:	The adsorption process is irreversible
$R_L=1$	:	Linear adsorption
$R_L>1$	:	Unfavorable adsorption
$0<R_L<1$	:	Favorable adsorption

2.5.2   Freundlich isotherm

The equations of the Freundlich isotherm can be using describe the both of chemical and physical adsorption. Accordingly, it can use to investigate the adsorption of organic and inorganic substances such as activated carbon, and synthetic resins. The Freundlich isotherm is developed from Langmuir isotherm that using for describe for heterogeneous adsorbent and the adsorption on the surface of the adsorbent will be multilayer. The Freundlich equation is shown below by Equation 2.3 and 2.4.

Freundlich equation: $\qquad Q_e = K_F C_e^{1/n}$
(2.3)

and $\qquad \qquad \qquad \log Q_e = \log K_F + \frac{1}{n} \log C_e$
(2.4)

where

C_e (mg/L) = the concentration of adsorbate at equilibrium

Q_e (mg/g) = the amount of adsorbate adsorbed at equilibrium

K_F (mg/g (mg/L) $^{1/n}$) = the Freundlich adsorption capacity parameter

n = the Freundlich adsorption intensity parameter

For the magnitude of n quantifies the favorability of adsorption and the degree of heterogeneity of adsorbate surface.

if   n=1 ;   the adsorption in constant

           n<1 ;   the adsorption strength decrease with the concentration of
                   solution increased

2.6   Literature reviews

2.6.1   Synthesis of Magnetic Carbon nanoparticles (M-CNPs)

Lee et al. [21] synthesized aligned carbon nanotubes (aligned CNTs) by co-pyrolysis of ferrocene and acetylene in the temperature range 700-1000°C. The diameter of CNTs is uniformly 10-30 nm at all temperature and the length of CNTs reaches to 3 mm at 1000°C. However, the size of the growing tube will be controlled by the size of the catalytic particle. And when the reaction temperature was increased the growth rate, the straight, and crystallinity of CNTs will be increased. The Arrhenius plot yields show that the activation energy is 35±3 kcal/mol, which is close to the diffusion energy of carbon in bulk γ-Fe.

Lupo et al. [13] synthesized of single-walled carbon nanotubes (SWCNTs) by spray pyrolysis of ferrocene and alcohol solution under an Ar atmosphere at 800-950°C. In this report, multi-walled carbon nanotubes (MWCNTs), small diameter 10-35 nm, was obtained in the hot zone of the reactor with a large number of 25 nm diameter metal perticles was also present (consisting of Fe). Some of the MWCNTs

were partially filled with Fe, and others contained metal particles at the ends. While SWCNTs bundles (diameter 3.5 nm) entangled to metal paricles (diameter 2-25 nm) was obtained at the worm zone outside the furnace. The optimum conditions for producing crystalline SWCNTs occurred at 950°C and as the ferrocene concentrations in ethanol solution increase (e.g., 1.2 wt %). In addition, ferrocene concentration have an influence to be metallic of the tubes.

Sano et al. [22] proposed to separately of Fe-included carbon nanocapsules (CNCs) and multi-wall nanotubes (MWCNTs) by using —fall-to-stop-reactor". The temperature were controlled in the range of 600-1000°C   and the flow rate of H$_2$ (carrier gas) was 100cm^3/min. The solid products would deposit consisting of Fe-included CNTs and CNCs. The products were obtained from differenced zone of the reactor that divides into five zones containing 500-600°C, 600-700°C, 700-800°C, 800-900°C and 900-1000°C. It found that at temperature was higher than 900°C the high yield of Fe-included CNTs and CNCs was obtained and at 1000oC was the optimized temperature to achieve the separated synthesis of CNTs and CNCs.

Chaisitsak et al. [23] synthesized of Single-walled carbon nanotubes by CVD method using silicon substrate as a support under atmospheric pressure. The reaction parameters such as furnace temperature in range 650-800°C, ratio between Ferrocene / Ethanol, flow rate of gas carrier (argon) and deposition time of the SWCNTs was found that the suitable position for the formation of SWCNTs is the worm region outside the furnace at a temperature of about 700°C. The diameter of CNPs was increased when the reaction temperature increased because a high temperature metal particle would collide with the other more. Then, CNTs have a larger diameter and the crystalline increased. For the ratio of Ferrocene / Ethanol, the optimum concentration for synthesis CNTs is 1.0 to 1.5% by weight of Ferrocene. The length and crystalline of CNTs tended to reduce as increasing the flow rate of carrier gas due to decrease of residence time.

Liu et al. [6] studied the different sublimation temperatures on the growth of different magnetic carbon nanostructures by pyrolysis of pure ferrocene. When

ferrocene was sublimated at 90°C, 130°C, 150°C and 280°C, it show Fe nanoparticles (Fe-NPs) adhering to single-walled carbon nanotubes (SWCNTs) which the metal oxide is mainly Fe_2O_3, carbon-encapsulated Fe-NPs with a core-shell structure of an iron core and carbon shell, Fe-NP decorated multi-walled carbon nanotubes (MWCNTs), and Fe-filled MWCNTs. Then the formation of carbon nanostructures can be controlled by adjusting the sublimation temperature of ferrocene. The magnetic characterization show that these nanostructures have an enchanced coercivity, higher than bulk Fe at room temperature.

Charinpanitkul et al. [24] synthesized carbon nanostructures by pyrolyzing of naphthalene as a carbon source and ferrocene as a catalyst metal with a molar ratio of 1:1 at synthesizing temperature of 800-1050°C. In this report, CNCs would prefer provide at elevated temperature while CNTs could preferably provide at lower temperature. The CNPs was contained with Fe nanoparticles inside their carbon shells. The production yield of synthesized CNPs have tendency increased when increasing temperature because the generation rate of carbon and Fe clusters would be more improved owing to the higher rate of decomposition.

Zhao et al. [25] synthesized multi-walled carbon nanotubes (MWCNTs) via the pyrolysis of ethanol by using Fe/MCM-41 as a catalytic template. The reaction temperatures ranging from 600-800°C was investigated. CNTs cannot be obviously when the reaction temperature is 600°C, when the temperature was increased to 700°C, the CNTs can grow but they are impure. At the reaction temperature was increased to 800°C, CNTs with open holes at the ends and of high purity can be obviously observed. But when the reaction temperature was further increased to 900°C, it was found a large amount carbon black. The optimum synthesizing temperature is about 800°C that show high purity with 18 concentric shells of graphite layers.

2.6.2 Application of M-CNPs on removal environmental pollution

Qu et al. [26] studied the removal of dyes (methylene blue and neutral red) from aqueous solution by using magnetic multi-walled carbon nanotubes. Fe_2O_3 nanoparticles were filled in multi-walled carbon nanotubes (MWCNTs) by wet chemical method. The magnetic MWCNTs played the surface area of $114m^2/g$ and $0.306cm^3/g$ of microporous volume. The effect of contact times on adsorption the dyes on to magnetic MWCNTs shown reaching the equilibrium only 60 min. The adsorption isotherm shown the maximum adsorption capacity for MB and NR were 42.3 and 77.5 mg/g, respectively and the freundlich isotherm was used to describe the equilibrium adsorption. After adsorption the magnetic MWCNTs showed the benefit in separation from dyes solution by external magnetic.

Gong et al. [5] investigated the remove of cationic dyes from aqueous solutions by using magnetic multi-wall carbon nanotubes (MMWCNTs). They studied the adsorption kinetics, adsorption capacities and pH. The specific surface area of MMWCNTs was 61.74 m^2/g that higher than MWCNTs (44.29 m^2/g). The mechanism of MMWCNTs adsorption for cationic dye might be based on van der Waals interactions between carbon atom in graphite sheet of MMWCNTs and aromatic backbones of dyes, and the other one was the electrostatic attraction between the positive charged of cationic dyes and the negative charged of MMWCNTs. Kinetic models could be well fitted by pseudo second-order models and the adsorption isotherms used freundlich model for described.

Tang et al. [27] studied the adsorption of atrazine and Cu (II) from wastewater by magnetic multi-walled carbon nanotube (MMWCNT). The specific surface areas of MMWCNT were $138.66m^2/g$ and the saturated magnetization of MMWCNT is 8.06emu/g. For adsorption kinetics, the effect of contact time on adsorption of atrazine by using MMWCNTs was found reaching equilibrium within 10 min and the adsorption capacity of atrazine reached 40.16 mg/g when the initial concentration of atrazine was 5 mg/L. For adsorption of Cu (II) shown reaching the equilibrium in 6 h and the adsorption capacity was 38.91 mg/g. The Freundlich isotherm indicated better

describes the adsorption of atrazine and Langmuir isotherm for adsorption of Cu (II). However, the regeneration of MMWCNT was evaluated by using 20% acidic ethanol solution at pH 3.

2.6.3 Application of M-CNPs on removal antibiotics

Jafari et al. [28] used MWCNTs as adsorbent for batch adsorption of two cephalosporins antibiotics (cephalexin and cefixime) from aqueous solution. They studied the influence of pH, sample volume, adsorbate and adsorbent concentration and temperature. The isotherm models explain by Langmuir isotherm for cephalexin and freundlich model for cefixime. The kinetics model could be well fitted of pseudo-first-order that showed higher R^2. Temperature did not have any effect on adsorption in this report. The maximum adsorption capacity of MWCNTs for adsorption of cephalexin and cefixime was 1100 and 820 mg/g, respectively.

Zhang et al. [29] studied the adsorption of olaquindox (OLA) on different types of carbon nanotubes (CNTs) which were pristine (MWCNT, Short-MWCNT), hydroxyl functionalized (MWCNT-OH, Short-MWCNT-OH) and carboxyl functionalized (MWCNT-COOH, Short-MWCNT-COOH). However, MWCNTs showed higher adsorption of OLA than Short-MWCNT, MWCNT-OH and MWCNT-COOH. Due to MWCNT adhered with each other that lead to have space between the bundles. Therefore, MWCNTs showed more adsorption sites than Short-MWCNT. For functional groups of MWCNT showed increase diffusional resistance including to the molecules of water could form H-bond with functional groups on MWCNT that covers the adsorption sites and blocks the OLA molecules to the adsorption sites.

Zhang et al. [2] investigated the adsorption efficiency of tetracycline (TC) on MWCNTs. The reaction parameter such as pH, ionic strength, adsorbent amount, sorption time and temperature was studied. The Influence of pH and ionic strength for remove TC on MWCNTs showed that could effectively remove in the range of pH 4.5-7.0 while ionic strength could hardly impact the adsorption of TC. The optimum adsorbent amount was 8.0 mg of MWCNTs which showed the adsorption percentage

was nearby 99.8%. Kinetic studied presented that the equilibrium was achieved in only 20 min, could be well fitted of pseudo-second-order models. While the Langmuir adsorption isotherm equations were studied that showed the maximum adsorption capacity of 269.54 mg/g at 293 K of TC on MWCNTs. The mechanism of adsorption is presumably the non-electrostatic π-π dispersion interaction and the hydrophobic interaction between TC and MMWCNTs.

Carabineiro et al. [30] studied on comparison the adsorption of ciprofloxacin (CPX) on three types of carbon-based materials consist of activated carbon, carbon nanotubes and carbon xerogel. It shown that the equilibrium was reached after 3 days with adsorption capacity of carbon xerogel and activated carbon were 112 and 231 mg/g, respectively. However, the Langmuir models was shown the best fitting. For the highest adsorption capacity per unit of surface area was occurred in CNT sample due to its electron-donor capacity.

Zhang et al. [31] investigated the adsorption of sulfamethoxazole (SMX) on functionalized carbon nanotubes to study the effect of cations (Ca^{2+}, Cs^{+}) and anions (phosphate). The important mechanism for SMX adsorption on CNTs was hydrophobic interaction and electrostatic interaction then the complication and ion pairs of SMX with metal ions could increasing the hydrophobicity and decreasing the electrostatic repulsion between SMX and negatively charged. Moreover, pH around 7.5 of CNT and the effect of adsorbed cations can increase SMX adsorption on CNTs.

Based on literature reviews, it might be suggested that the magnetic carbon nanoparticles, which was synthesized by co-pyrolysis of ethanol and ferrocene, can be applied as a promising novel solid adsorbent for removal the antibiotics in wastewater. In addition, it could be easily separated from the aqueous solution by permanent magnetic due to its magnetic properties.

CHAPTER III

EXPERIMENT

This chapter describes the experimental procedures based on some literatures surveys. The following experimental procedures are designed as a guideline for obtaining consistent results. Experimental works would be divided into 2 parts; which are (1) Synthesis of Magnetic carbon nanoparticles (M-CNPs) by co-pyrolysis, (2) Adsorption of antibiotics on synthesized M-CNPs.

3.1 Experimental setup for synthesis of Magnetic carbon nanoparticles (M-CNPs) by co-pyrolysis of ethanol and ferrocene
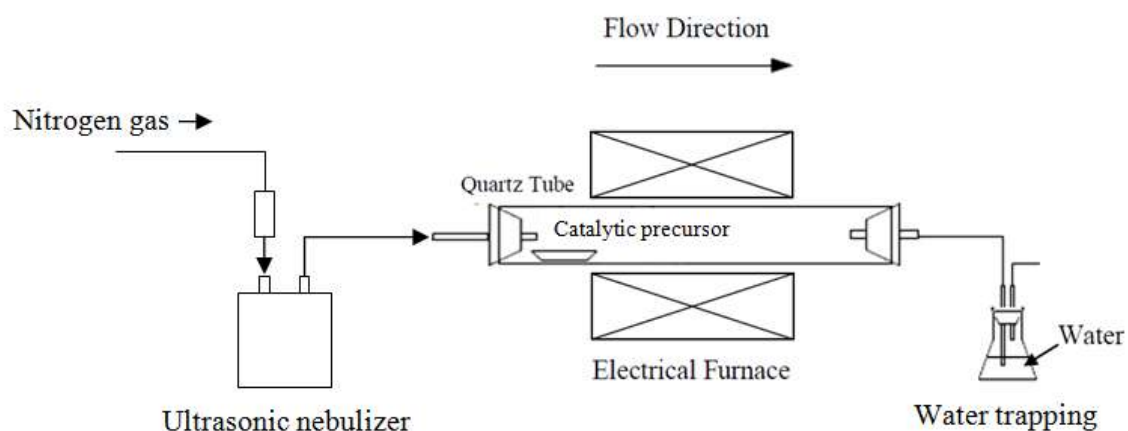
Figure 3.1 Schematic diagram of experimental set up for co-pyrolysis using ethanol and ferrocene.

The schematic diagram of experimental apparatus has shown in Figure 3.1. For synthesizing of M-CNPs, ethanol (C_2H_5OH) and ferrocene (Fe (C_5H_5),) are used as a carbon source and catalytic precursor, respectively. The experimental setup consisted of an ultrasonic nebulizer (Figure 3.2), a mist carrying, an electrical furnace (Figure 3.3), a quartz tube (inner diameter of 4.2 cm and length of 60 cm), a ceramic

boat of precursor, silicone plugs and a water trapping. Table 3.1 revealed the list of chemical agents that used for synthesis M-CNPs.

Table 3.1 List of chemical agents used in this research in the part of synthesized M-CNPs

Chemical agents	Manufacturer / Grade / Properties
Ethanol absolute (C_2H_5OH)	VWR International S.A.S / 99.8% purity / Boiling point: 78.1^oC
Ferrocene ($Fe(C_5H_5)$)	Sigma-Aldrich / 98 % purity / Boiling point: 249^oC
Nitrogen (N_2)	Thai Industrial Gas Public Company Limited (TIG) / Ultra high purity 99.99% purity

Figure 3.2 An ultrasonic nebulizer (NE-U17, Omron)

Figure 3.3 Electrical furnace

Figure 3.4 Automatic temperature controllers

3.2 Synthesis of Magnetic carbon nanoparticles (M-CNPs) by co-pyrolysis of ethanol and ferrocene[23]

For measuring temperature profile of the quartz tube reactor, temperature profile in the range of 700-900°C was measured by using an automatic temperature controller as shown in Figure 3.4. The Ethanol as a carbon source would be put in the cup of ultrasonic nebulizer, while ferrocene are loaded into a ceramic boat, which is placed in the quartz tube inside the electrical furnace where the temperature was high enough for vaporization of the precursor. The ferrocene to ethanol ratio was varied in the range of 7 wt% - 9 wt% of ferrocene relative to ethanol. The furnace temperature was conducted set controlling in range 700-900°C. After the furnace was being heated from room temperature to the desired temperature and was stable, the ultrasonic nebulizer was turned on and creating a small droplet of ethanol. The droplet generator was based on an electrical ultrasonic nebulizer (ultrasonic frequency of 1.7 MHz). The droplet average diameter was estimated to be about 2.1 μm using the Lang's Equation 3.1.

$$D_d = 0.34(\frac{8\pi\gamma}{\rho f^2})^{1/3}$$
(3.1)

where

D_d = Droplet diameter (μm)

γ = Solution surface tension (21.55×10^{-3} N/m for pure ethanol)

ρ = Solution density (789 kg/m^3 for pure ethanol)

f = Ultrasonic frequency (1.7 MHz)

After that, the small droplet of ethanol was introduced into the quartz tube by lead of carried gas (nitrogen) which carried out of 2 L/min at all experiments. The process was controlled for 45 min, afterwards the reactor gradually cooled down to room temperature and the synthesized black products was obtained on inner wall of

the quartz tube. After that these synthesized black products were collected and characterized their properties and using in adsorption of antibiotics part.

3.3 Experimental setup for adsorption of antibiotics on synthesized M-CNPs

The experimental procedures for antibiotics sorption onto synthesized M-CNPs are conducted in batch system. The influence parameters such as the amount loading of adsorbent, pH solution, adsorption kinetics and adsorption isotherm were studied. The wavelength at the maximum absorbance of typical antibiotics solution will be measured by UV-VIS Spectrophotometer. The photograph of experiment setup for batch adsorption as reveals in Figure 3.5 that consisted of a temperature controller, a glass bottle with aluminium foil covered, a water jacket for control temperature and a magnetic stirrer.

Figure 3.5 The photograph of batch system for adsorption experiment.

This research is concentrated on the adsorption of tetracycline ($C_{22}H_{24}N_2O_8$) by using M-CNPs. For structure and properties of tetracycline was played in Figure 3.6.
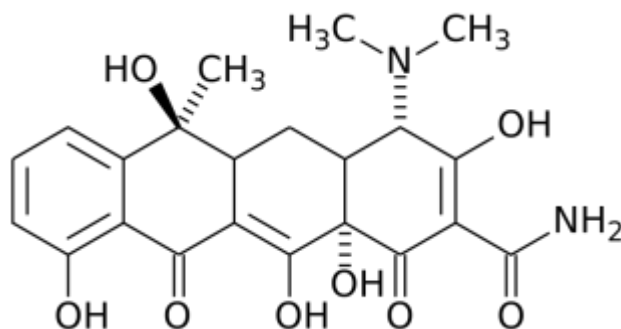
Chemical agents	Manufacturer / Grade / Properties
Tetracycline (TC) ($C_{22}H_{24}N_2O_8$)	Sigma Aldrich Co. / ≥ 98% / MW (444.44 g/mol)

Figure 3.6 Structure and properties of tetracycline

3.4   Experimental procedures for adsorption of antibiotics on synthesized M-CNPs

3.4.1   Preparation of typical antibiotic solutions

Typical antibiotic solution of tetracycline was prepared by dissolving the tetracycline powder in de-ionized water at the design concentration. The wavelength of maximum absorbance was measured by UV-vis spectrophotometer which detected in the visible range of 200 to 500 nm. The standard curve of tetracycline as shown in an Appendix A.

3.4.2 Batch experiment for adsorption tetracycline onto M-CNPs

All experiments were conducted in batch system which the experimental setup as shown in Figure 3.5. The bottle glass was covered with aluminium foil to protect the light then typical tetracycline solution would be added in the glass bottle which was stirred about 10 min, the sampling at the initial time was taken for measuring an absorbance. M-CNPs would be filled in this solution which was continually stirred until reaching equilibrium after that the sampling was taken at different time. An adsorbent (M-CNPs) in sampling were separated from typical solution by external permanent magnet and syringe filter. The concentration of typical solution after adsorption was measured by UV-vis spectrophotometer. In this research, batch experiment could be divided into 4 parts consists of the studies of the amount loading of M-CNPs, initial pH value, adsorption kinetics and adsorption isotherms. The variables of the adsorption experiments were shown in Table 3.2.

Table 3.2 The variables of the adsorption experiments

Studies	Variables				
	Initial TC concentration (mg/L)	Amount of M-CNPs (mg per 25 mL)	Initial pH value	Temperature (^{o}C)	Contact time (min)
The amount loading of M-CNPs	30	2-12	7±0.5	25±1	600
pH value	30	8	1-11	25±1	600
Adsorption kinetics	30	8	7±0.5	25±1, 45±1 and 65±1	Until reaching equilibrium
Adsorption isotherms	10-100	8	7±0.5	25±1, 45±1 and 65±1	600

3.4.2.1 Effect of the amount of adsorbent (M- CNPs) loading

For investigating on the amount of adsorbent (M-CNPs) loading, the experiments were conducted in 100 mL of glass bottle. The amounts of M-CNPs in range of 2-12 mg per 25 mL of solution were dispersed in the typical solution with initial TC concentration of 30 mg/L. The temperature and pH value were controlled at $25\pm1^{o}C$ and 7 ± 0.5 (pH value of de-ionized water), respectively. The experiments were carried out 600 min after that the sampling of typical solution was collected for measure an absorbance.

3.4.2.2 Effect of initial pH value

The effect of initial pH value was varied from 1 to 11 with the initial TC concentration of 30 mg/L and 8 mg of M-CNPs loading per 25 mL of solution. In this study, all experiments were conducted in 100 mL of typical solution and the temperature was controlled at $25\pm1^{o}C$. For adjusting the pH value, 0.1M of NaOH and HCl were used by adding in the de-ionized water until reaching the require pH value then the powder of TC was dissolved in adjusted solution at 30mg/L.

3.4.2.3 Adsorption kinetics

The adsorption experiments were carried out using 1000 mL of glass bottle containing 8 mg of M-CNPs loading per 25 mL of typical solution with the initial TC concentration of 30 mg/L at pH value about 7 ± 0.5. The temperature was investigated from 25, 45 to $65^{o}C$. The sampling of typical solution was taken in 4 mL at different time until 24 hr to find the equilibrium time after that the M-CNPs were separated from the sampling by external permanent magnet and syringe filter then the concentration of typical solution after adsorption was measured by UV-vis spectrophotometer.

3.4.2.4 Adsorption isotherms

Adsorption isotherms were investigated at different temperature and initial TC concentration. The temperature was varied from 25, 45 to 65°C and initial TC concentration in the range of 10-130mg/L. The amount of M-CNPs loading was 8 mg per 25 mL of typical solution that conducted in 100mL at pH value of 7±0.5.

3.5   Analytical Instruments

The morphology of synthesized M-CNPs was analyzed by scanning electron microscopy (SEM) and transmission electron microscope (TEM) for synthesized M-CNPs morphology. For structure and chemical composition of synthesized M-CNPs, X-ray diffraction (XRD) and energy dispersive X-ray spectroscope (EDS) were used to analysis. Raman spectroscopy was performed the crystallinity of synthesized M-CNPs compared with the disorder. The surface charge properties and size of synthesized M-CNPs were analyzed by Zetasizer. BET was used to determine of the surface area and pore structure of synthesized M-CNPs. In addition, Fourier Transform Infrared (FT-IR) spectrometer was used to investigate the functional groups on synthesized M-CNPs and thermal gravimetric analyzer (TGA) for their thermal stability to comparison the M-CNPs after adsorption. For measuring the absorbance of typical solution, UV-vis spectroscopy was used to analysis. The details of analytical instruments were performed below.

3.5.1   Scanning Electron Microscopy (SEM)

The morphology of synthesized M-CNPs was investigated by using Scanning Electron Microscopy (SEM, JEOL: model JSM-5800LV) with energy dispersive X-ray spectroscope (EDS) as shown in Figure 3.7 at Scientific and Technological Research Equipment Centre Foundation, Chulalongkorn University. The powder of synthesized products were dispersed on carbon tape and loaded into the sample chamber and then the image would be shown.

Figure 3.7 Scanning Electron Microscope (SEM)

3.5.2 Energy Dispersive X-ray Spectroscopy (EXS)

For energy dispersive X-ray spectroscope which shown the elemental composition of synthesized products attached to the SEM.

3.5.3 Transmission Electron Microscope (TEM)

Structures of the synthesized products were investigated by TEM (JEOL model JEM 2100), operated at 80-200 KV accelerating voltage at Faculty of Science, Mahidol University. A photo of the Transmission Electron Microscope (TEM) is shown in Figure 3.8.

Figure 3.8 Transmission Electron Microscope (TEM)

3.5.4 X-Ray Diffraction (XRD)

X-ray diffraction (Bruker model AXS) was used to characterize the structure and composition of synthesized products at Faculty of Science, Chulalongkorn University. A photo of the X-ray diffraction was shown in Figure 3.9 that detected in a 2θ range of 20-80° with the step size of 0.02^o/min for synthesized product.

Figure 3.9 X-Ray Diffraction (XRD)

3.5.5 Raman Spectroscope

The crystallinity and disorder or defect of the synthesized products was characterized by Raman Spectroscope (DXR SmartRaman, Thermo Scientific) at Excellence in Particle and Technology Engineering laboratory, Chulalongkorn University as shown in Figure 3.10.

Figure 3.10 Raman Spectroscope

3.5.6   Zetasizer

For investigating the surface charge of synthesized products, zetasizer (ZETASIZER 300HSA) as shown in Figure 3.11 was used to characterize. The preparation for measurement the synthesized products would be dispersed in de-ionized water which adjust pH value at the requirement for studies of the charge of products at different pH value. Moreover, this measurement could be obtained the size of synthesized products by Dynamic Light Scattering (DLS).

Figure 3.11 Zetasizer

3.5.7 Brunauer-Emmett-Teller (BET) analyzer

The surface area and porous structure of synthesized products were analyzed by using Brunauer-Emmett-Teller (BET) analyzer (BEL model BELSORP-mini, Japan) at Excellence in Particle and Technology Engineering laboratory, Chulalongkorn University as shown in Figure 3.12. The process was carried out by nitrogen adsorption-desorption at liquid nitrogen temperature (77 K). The synthesized products about 0.2 g were pretreated at 150°C for removals contaminate and moisture under vacuum for 4 hours before analysis.

Figure 3.12 Brunauer-Emmett-Teller (BET) analyzer

3.5.8 UV-Visible Spectrophotometer (UV-Vis)

The UV-Vis spectrophotometer (Shimadzu model UV-1700) at Excellence in Particle and Technology Engineering laboratory, Chulalongkorn University was used to measure absorbance of the typical tetracycline solution. The wavelength of 200-500 nm was detected in this study. A photo of the UV-Vis spectrophotometer was shown in Figure 3.13.

Figure 3.13 UV-Visible Spectrophotometer (UV-Vis)

CHAPTER IV

RESULTS AND DISCUSSION

4.1 Synthesis of magnetic carbon nanoparticles (M-CNPs)

This part is dedicated to investigation on effect of synthesizing temperature and weight ratio of ferrocene to ethanol on characteristics of synthesizing magnetic carbon nanoparticles which would be employed for adsorption antibiotic contaminated in wastewater.

The synthesizing temperature was varied in the range of 700, 800 and 900°C with the weight ratio of ferrocene to ethanol of 7, 8 and 9wt%. Scanning electron microscopy (SEM), raman spectroscopy, BET analysis, yields of synthesized M-CNPs and the adsorption efficiency (%) of M-CNPs have been examined for figuring out the characteristics of the synthesized M-CNPs.

4.1.1 Temperature profile within quartz tube reactor

An electrical furnace and a quartz tube reactor were employed for synthesizing magnetic carbon nanoparticles by co-pyrolysis between ethanol and ferrocene. The quartz tube with inner diameter 42 mm and outer diameter 4.6 mm was inserted into the furnace of which temperature was controlled in the range of 700-900°C. A thermocouple was put into the quartz tube along its axial distance of every 2 centimeters while temperature of the furnace was increased from room temperature to the designated temperature, as shown in Figure 4.1.

Temperature distribution along the axial distance achieves a maximum at the middle zone and becomes lower at both ends. A ceramic boat with loaded ferrocene was placed into the quartz tube at the position of which temperature is higher than 250°C, resulting in the vaporization of ferrocene (13, 11 and 10 cm from inlet where the desired temperature was 700, 800 and 900°C, respectively). After the maximum temperature achieves the set point temperature the ultrasonic nebulizer was turned on

to generate small droplets of ethanol that was introduced into the quartz tube by constant nitrogen gas flow rate of 2L/min. Each experiment was conducted for 45 minutes. The synthesized black products were collected from the inner wall of the quartz tube which was categorized into 3 zones (the front zone (0-15 cm from inlet), the middle zone (15-45 cm from inlet) and the end zone (45-60 cm from inlet)). The synthesized products were characterized by SEM, TEM, XRD, FT-IR, BET, Raman spectroscopy and zeta potential analyzer for finding relationship among those characteristics and the synthesizing conditions.
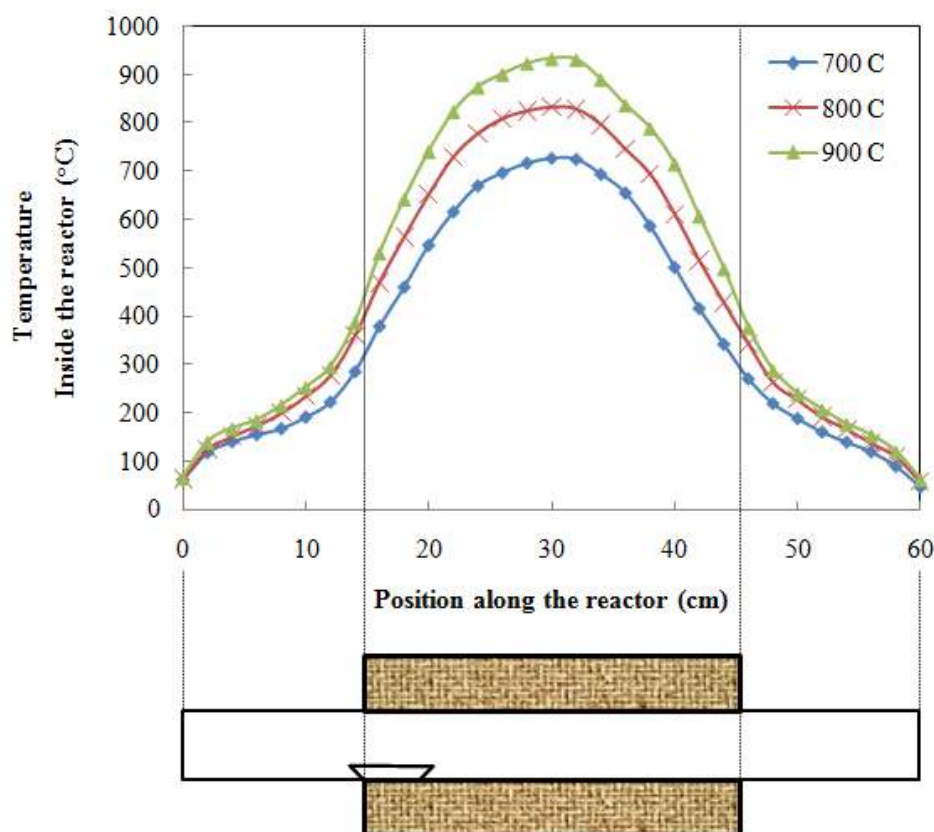
Figure 4.1 Temperature profile along the axial direction of the quartz tube reactor

4.1.2 SEM analysis of synthesized M-CNPs

The microscopic structure of synthesized black products collected from the inner wall of the quartz tube by scanning electron microscopy (SEM). Three zones which are the front zone (0-15 cm from inlet), the middle zone (15-45 cm from inlet) and the end zone (45-60 cm from inlet) were taken into account with respect to the local temperature.

The synthesized products collected from the front zone mainly consist of agglomeration of amorphous. This result would be ascribed to incomplete self-assembly of carbon precursor regardless the synthesizing temperatures (700, 800 and 900°C) and ratio of ferrocene to ethanol (5, 7, and 9wt %). Figure 4.2 illustrates SEM micrographs of synthesized products. Typical SEM micrograph in Figure 4.2 (a) reveals that the synthesizing products with the synthesizing temperature of 700°C exhibit spherical morphology with nominal diameter of 30-50 nm. An increase in the synthesizing temperature to 800 and 900°C exert insignificant effect on morphology and size of the synthesizing products. Similarly, an increase in weight ratio of ferrocene to ethanol to 7 and 9 wt% gives rise to an insignificant effect on morphology and size of the synthesized products. However, it was found that when the synthesizing temperature was increased the agglomeration of particles became more enhanced regardless of ratio of ferrocene to ethanol.

It could be observed that the synthesized products collected from the middle zone consist of a large amount of carbon nanotubes (CNTs) with only few agglomerations of amorphous carbon nanoparticles. With the synthesizing temperature of 700°C, the as-grown CNTs exhibit nominal diameter of 40-50 nm regardless of weight ratio of ferrocene to ethanol as shown in Figure 4.3 (a-c). With the increase in the synthesizing temperature to 800 and 900°C, a gradual increase in the diameter of as-grown CNTs could be observed. The average diameter of the synthesizing CNTs was increased from 40-50 to 40-60 and 50-500 nm with respect to the synthesizing temperature of 700, 800 and 900°C, respectively.

Synthesizing temperature		
700°C	800°C	900°C

Figure 4.2 SEM analysis of synthesized products at the front zone (a-c) at 5wt% (d-f) at 7wt% and (g-i) at 9wt% with the synthesizing temperature was 700, 800 and 900°C, respectively.

The nominal diameter of the as-grown CNTs was affected by the ratio of ferrocene to ethanol which was increased from 5wt% to 9wt%, as shown in Figure 4.3 (d-f). Figure 4.3 (g-i) illustrates the as-grown CNTs at the synthesizing temperature was 900°C with diameter of 50-500nm and several microns of length, however the extremely diameter was found at the ratio of ferrocene to ethanol was 9wt%. From previous researches, it could be indicated that the formation of carbon nanotubes due to the decomposition of ferrocene and ethanol and were lead into the middle zone by

nitrogen gas where self-assembling by diffusion of vapor of ethanol into the iron cluster catalyst that was emitted from decomposition of ferrocene, so the catalytic growth reactions could be take place and carbon nanotubes were formed [24, 32]. The effect of synthesizing temperature revealed at the higher temperature, the size of iron cluster catalyst became larger due to the iron nanoparticles were collided with other and coalescence to be the larger iron nanoparticles that would be the seed for formation of CNTs with large diameters at the higher synthesizing temperature [33].

Figure 4.3 SEM analysis of synthesized products at the middle zone (a-c) at 5wt% (d-f) at 7wt% and (g-i) at 9wt% with the synthesizing temperature was 700, 800 and 900°C, respectively.

Figure 4.4 (a-i) revealed the synthesized products deposited at the end zone containing the agglomerated carbon nanocapsules (CNCs) with iron nanoperticles of all condition that could be indicated when the synthesizing temperature was 700°C the CNCs with 30-60 nm diameters would be obtained of all ratio of ferrocene to ethanol and the diameter of CNCs would be increased to 40-60 nm and 60-100 nm when the synthesizing temperature was 800 and 900°C, respectively..
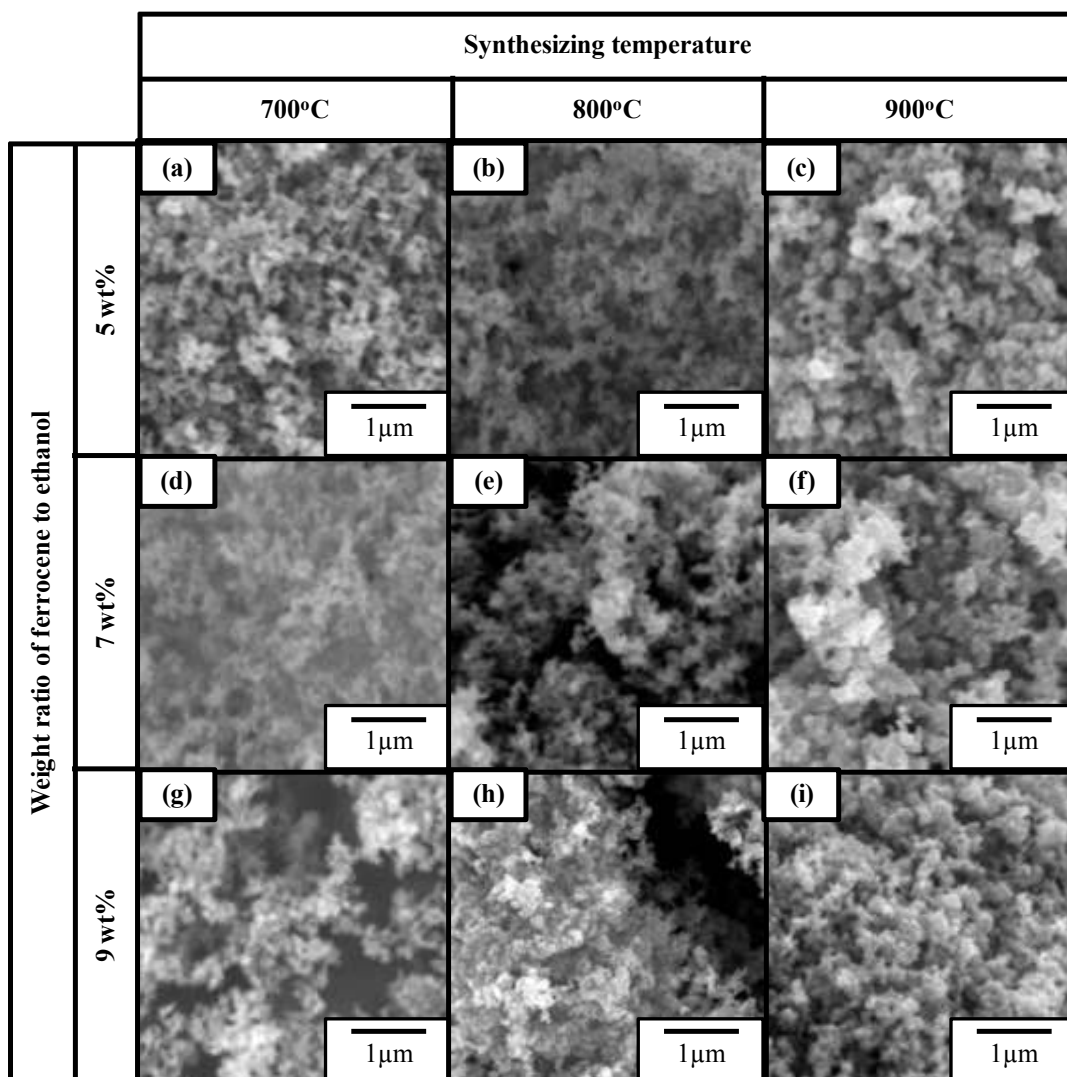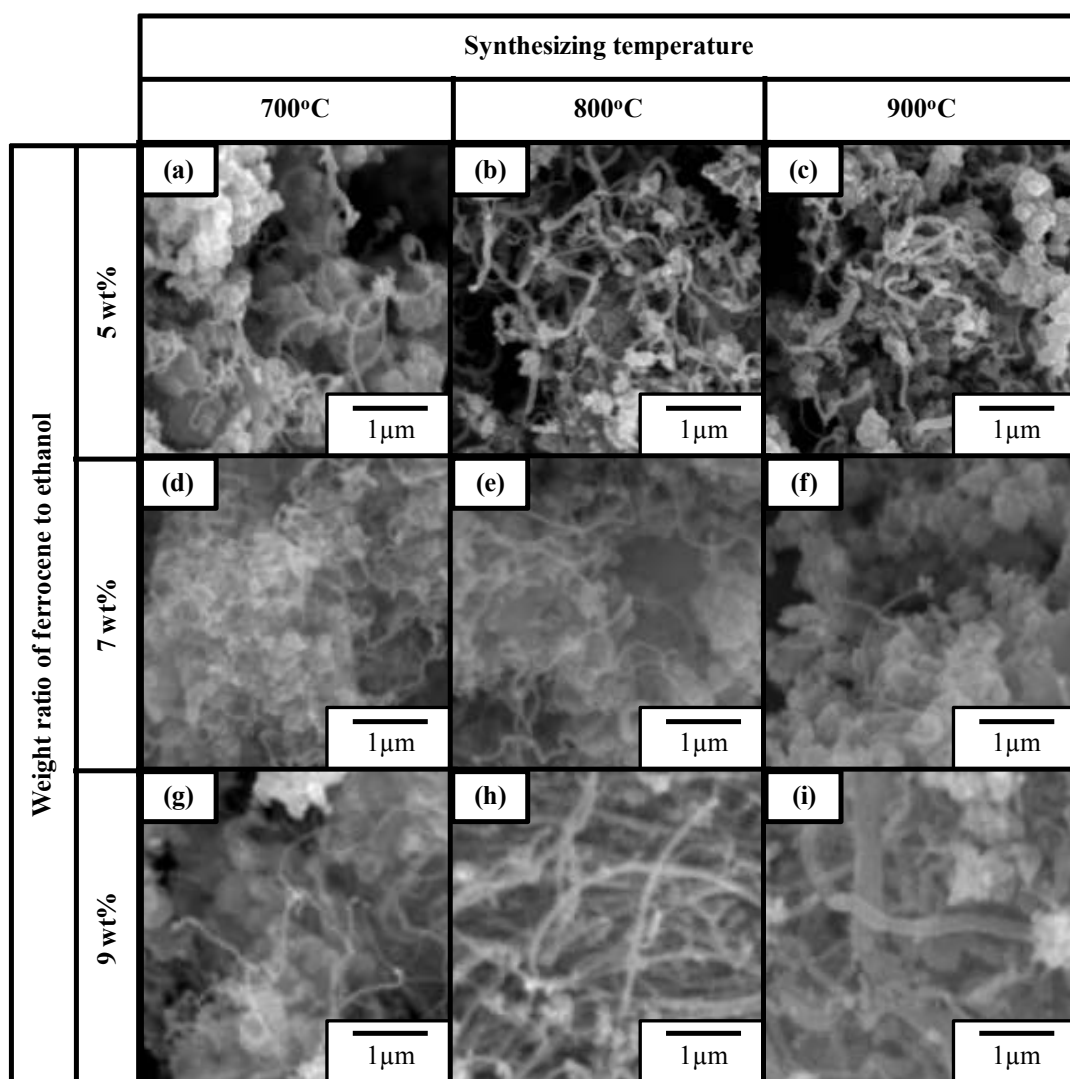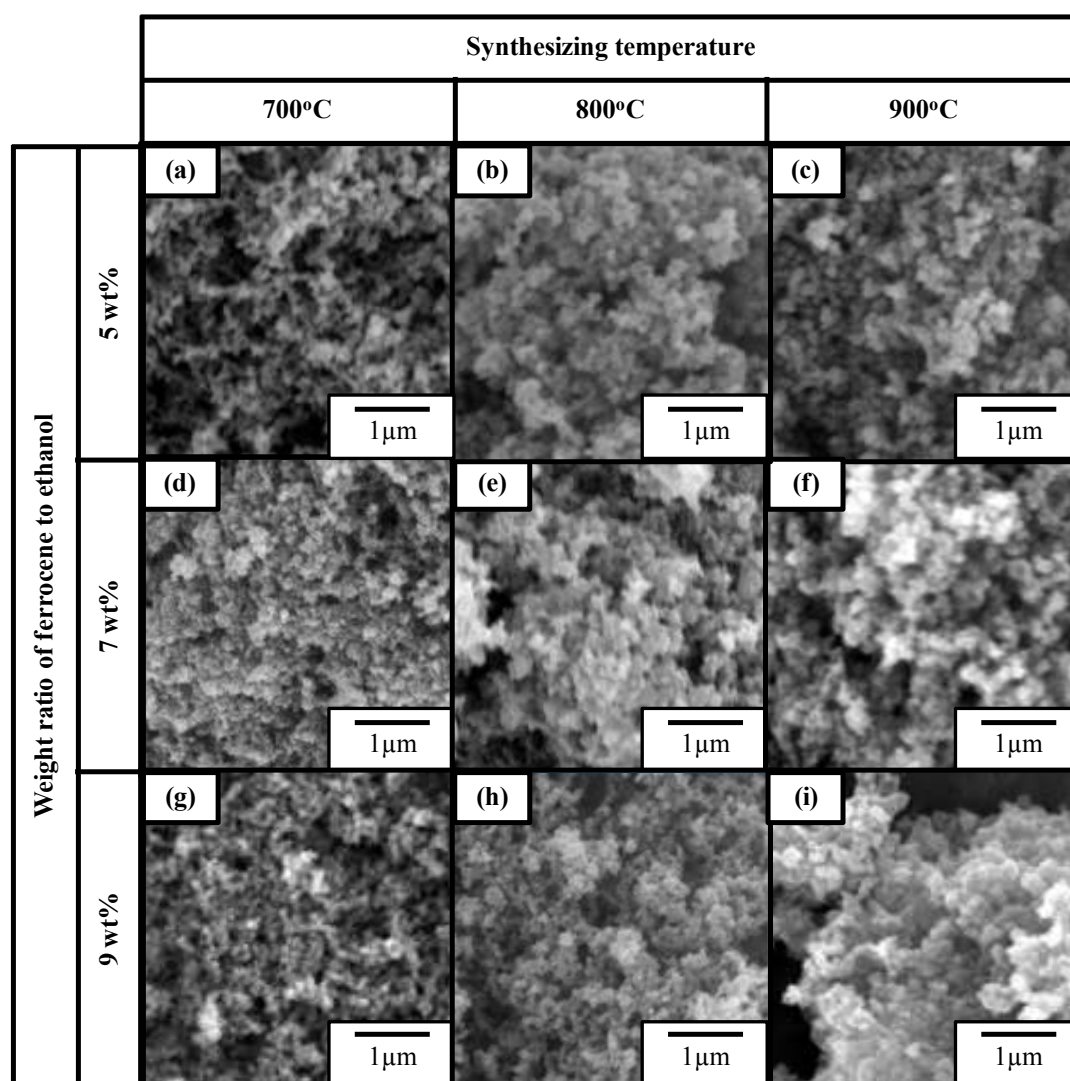

Figure 4.4 SEM analysis of synthesized products at the end zone (a-c) at 5wt% (d-f) at 7wt% and (g-i) at 9wt% with the synthesizing temperature was 700, 800 and 900°C, respectively.

However, the higher synthesizing temperature and higher ratio of ferrocene to ethanol the obtained products could be gathered more thickly and larger diameter. From previous research, the CNCs were formed when the carbon source were not continuously diffused to the iron cluster catalyst and the concentration of carbon source was not high enough [22, 34]

4.1.3 Raman spectrum of synthesized M-CNPs

In order to study of graphitic structure and disorder structure of synthesized magnetic carbon nanoparticles (M-CNPs), the synthesized products in the middle and the end zone were mixed and analyzed by Raman spectroscopy. It could be noticed that the samples exhibit distinctive peaks at 1,350 cm^{-1} and 1,580 cm^{-1}, which represent disorder carbon structure (D peak) and graphitic structure (G peak), respectively. Ratio of peak intensity (I_D/I_G) would be employed for determining the relative amount of amorphous to crystalline carbon nanostructures within the synthesized samples [21, 35]. Figure 4.5 illustrates Raman spectrum of the synthesized M-CNPs synthesized with 5wt% of ferrocene to ethanol. I_D/I_G of M-CNPs synthesized at the synthesizing temperature of 700, 800 and 900°C is 0.78, 0.64 and 0.39, respectively. As shown in Figure 4.6 I_D/I_G of the M-CNPs synthesized at synthesizing temperature of 700, 800 and 900°C were 0.94, 0.58 and 0.56, respectively. Similarly, Figure 4.7 revealed Raman spectrum of the M-CNPs synthesized with 9wt% of ferrocene to ethanol at 3 synthesizing temperatures. I_D/I_G of such M-CNPs synthesized at synthesizing temperature of 700, 800 and 900°C were 0.73, 0.68 and 0.47, respectively. However, all results suggested that synthesis of crystalline M-CNPs from mixture would be more prevalent than amorphous portion. I_D/I_G of all synthesized M-CNPs increases linearly with synthesizing temperature[21]. However, the M-CNPs synthesized at 900 ºC would contain the highest graphitic crystallinity because the self-assembling process of crystalline M-CNPs would be more enhanced at a higher temperature.
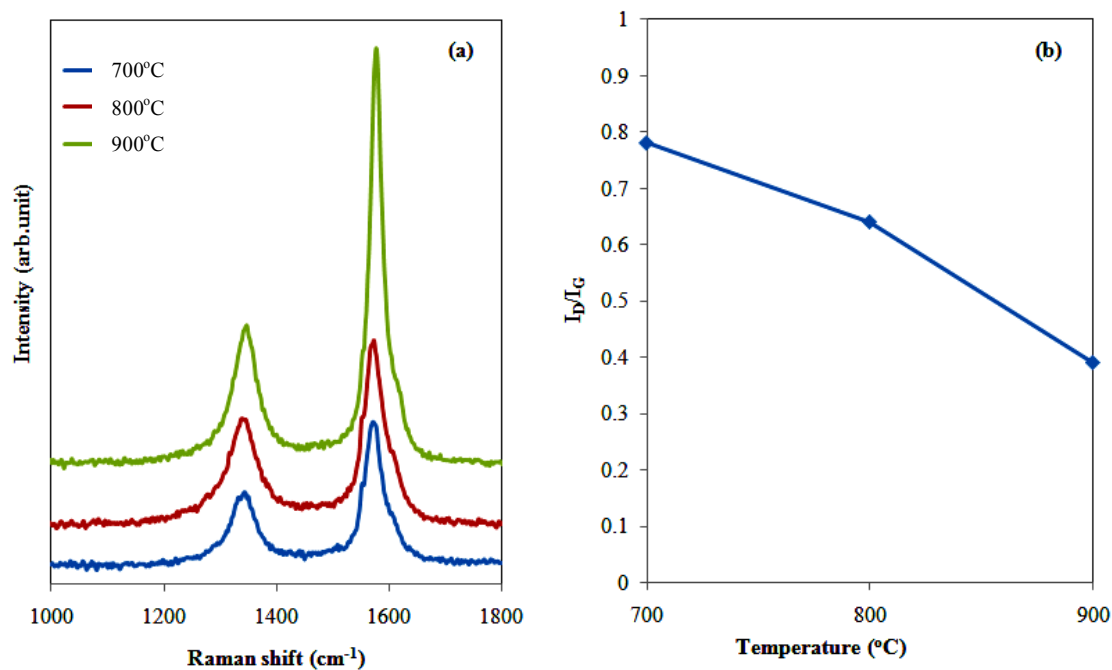
Figure 4.5 (a) Raman spectrum for the synthesized M-CNPs at synthesizing temperatures 700, 800 and 900°C. (b) Plot of I_D/I_G vs. synthesizing temperature at 5wt% ferrocene to ethanol.
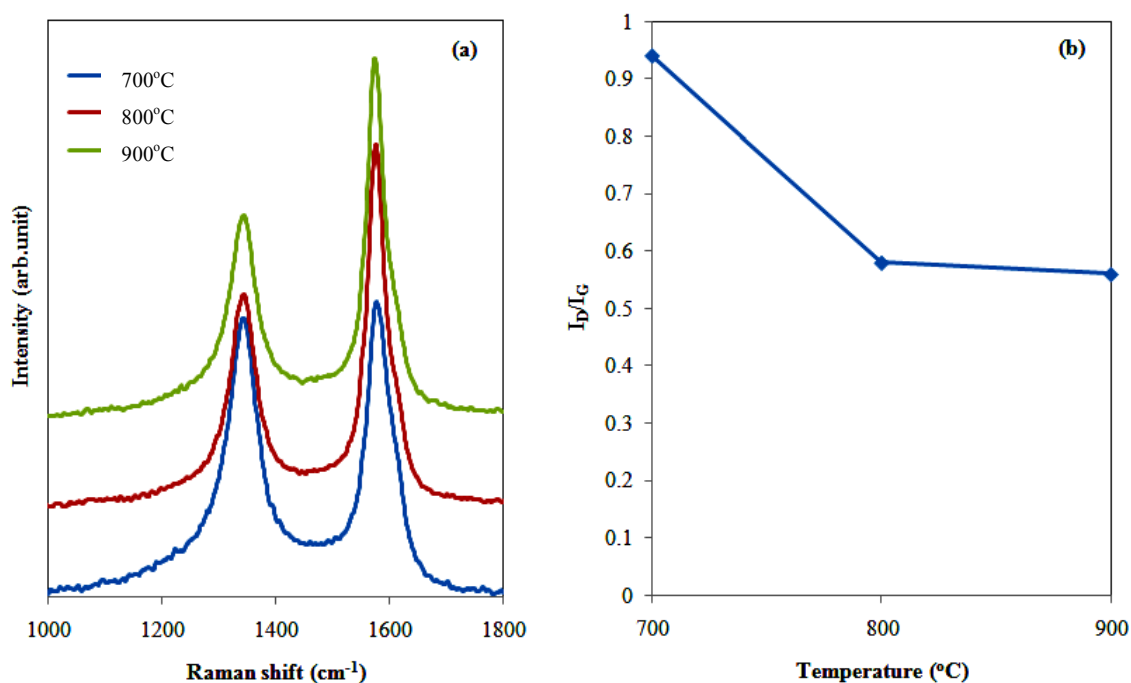
Figure 4.6 (a) Raman spectrum for the synthesized M-CNPs at synthesizing temperatures 700, 800 and 900°C. (b) Plot of I_D/I_G vs. synthesizing temperature at 7wt% ferrocene to ethanol.
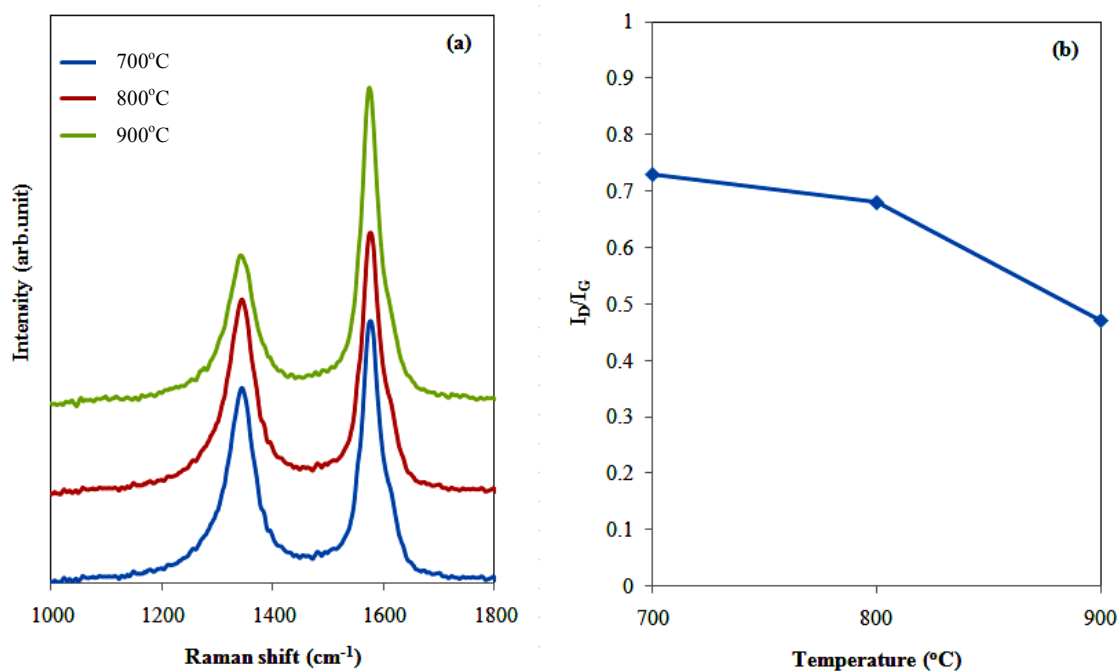
Figure 4.7 (a) Raman spectrum for the synthesized M-CNPs at synthesizing temperatures 700, 800 and 900°C. (b) Plot of I_D/I_G vs. synthesizing temperature at 9wt% ferrocene to ethanol

4.1.4 Surface area of synthesized M-CNPs analyzed by BET analysis

Surface area of synthesized M-CNPs, which were collected from the middle zone and the end zone, was analyzed by BET analysis as shown in Figure 4.8-4.10. It could be observed that when the synthesizing temperature was decreased the surface area would become higher. This BET result is consistent with the results of SEM analysis revealing that the smaller M-CNPs would be synthesized with the lower synthesizing temperature. Specific surface area of M-CNPs synthesized with 5wt% of ferrocene to ethanol at the synthesizing temperatures of 700, 800 and 900°C were 40.54, 38.50 and 24.04m²/g, respectively. With the higher ferrocene to ethanol ratio of 7wt%, the surface area of M-CNPs prepared at the synthesizing temperatures of 700, 800 and 900°C were 39.33, 36.21 and 28.41m²/g, respectively. Similarly, the surface area of M-CNPs synthesized from 9wt% of ferrocene to ethanol with the synthesizing

temperature of 700, 800 and 900°C were 47.12, 38.98 and 27.31m^2/g, respectively. Based on the comparison, the BET surface area of M-CNPs decreased significantly with the higher synthesizing temperature while the ratio of ferrocene to ethanol exerted insignificant effect on the BET surface area of M-CNPs.
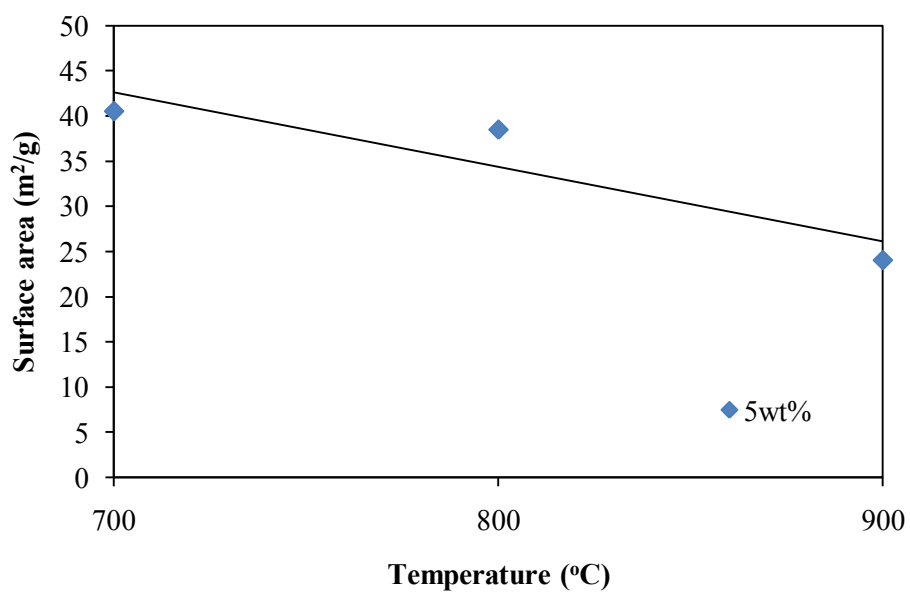
Figure 4.8 Surface area (m^2/g) of synthesized M-CNPs at 5wt% of ferrocene to ethanol
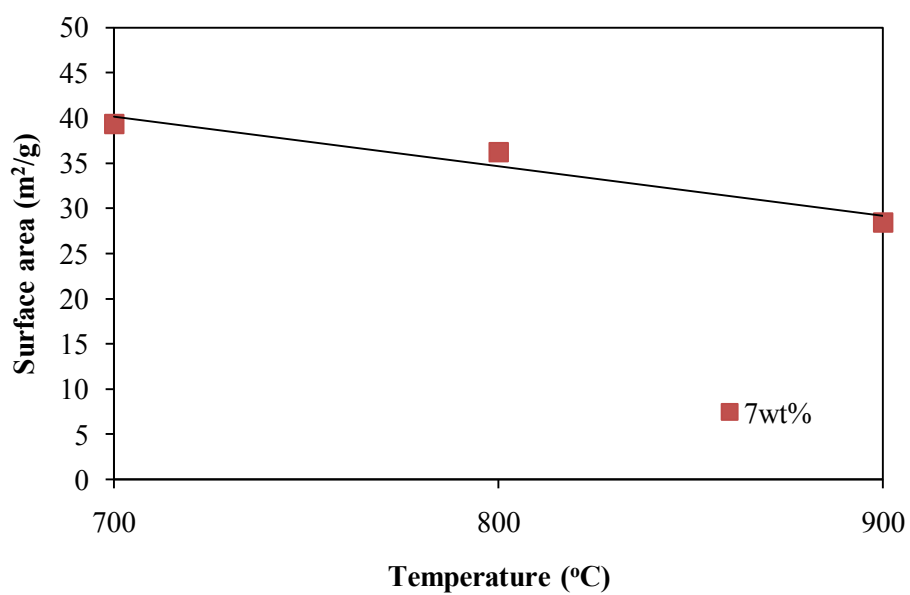
Figure 4.9 Surface area (m^2/g) of synthesized M-CNPs at 7wt% of ferrocene to ethanol
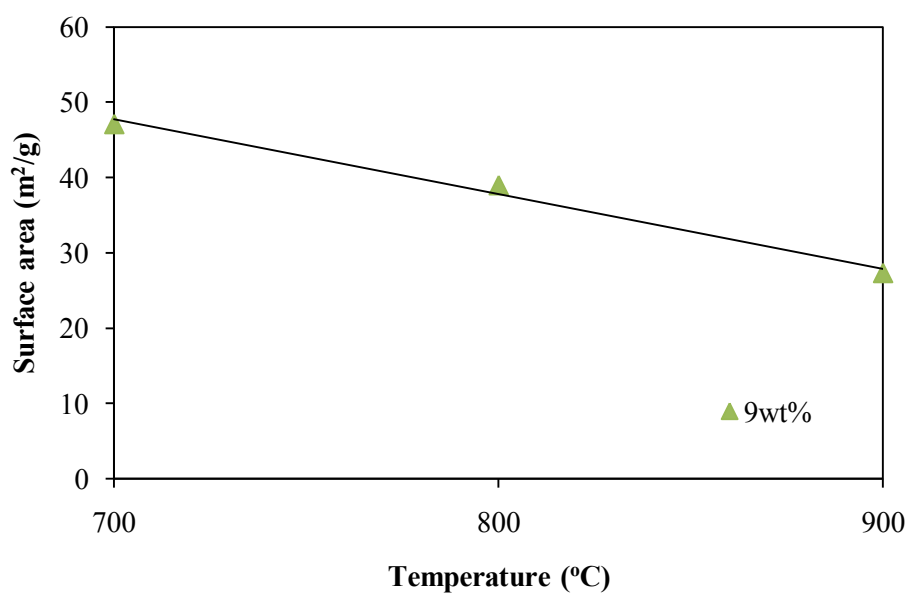
Figure 4.10 Surface area (m^2/g) of synthesized M-CNPs at 9wt% of ferrocene to ethanol

4.1.5 Carbon yield of synthesized M-CNPs

Carbon yields of the synthesized M-CNPs could be described in equation 4.1.

$$Carbon\ yield\ (\%) = \frac{W_{c,(middle+end)}}{W_{c,ethanol}+W_{c,ferrocene}} \times 100 \qquad (4.1)$$

where

$W_{C,(middle+end)}$ = Weight of synthesized carbon at middle and end zone

$W_{C,ethanol}$ = Weight of carbon in ethanol that was used

$W_{C,ferrocene}$ = Weight of carbon in ferrocene that was used

Figure 4.11 illustrates the percent of carbon yields of the synthesized M-CNPs at different synthesizing temperatures when the weight ratio of ferrocene to ethanol was 5, 7 and 9 %. When the ratio of ferrocene to ethanol was 5wt% at synthesizing temperatures was increased from 700 to 800 and 900 ºC, the carbon yield was increased from 0.86 to 1.78 and 4.12 %, respectively. At 7wt% of ferrocene to ethanol the carbon yield was 3.13, 6.61 and 6.68 % for synthesizing temperature was 700, 800 and 900ºC, respectively. And the last ratio that 9wt% of ferrocene to ethanol at synthesizing temperatures was increased from 700 to 800 and 900 ºC, the carbon yield was increased from 6.70 to 8.10 and 9.21 %, respectively. As also investigated by Lee et al., 2002 [36] suggested that the increasing of synthesizing temperature could boost the reaction rate of formation of CNTs which affected to their morphology and yields. Moreover, the increasing of weight ratio of ferrocene to ethanol affected to carbon yield, in the formation of carbon nanoparticles which consisted of diffusion and precipitation if the concentration of carbon atoms was too much the diffusion was much faster than the precipitation leaded to the remaining carbon atoms could not dissolve into catalyst particles, so the carbon nanoparticles could not formed. Then the higher weight ratio of ferrocene to ethanol, the carbon yield was increased.
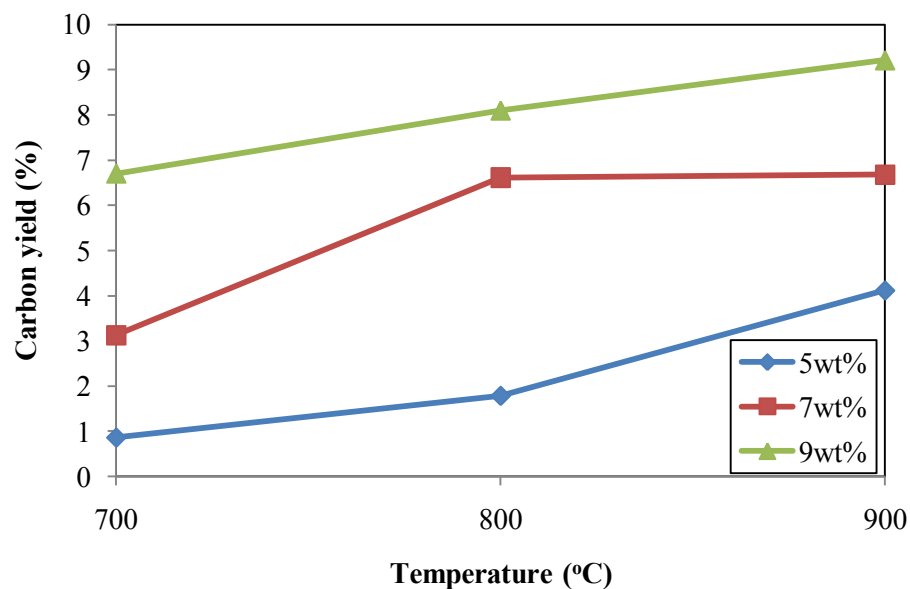
Figure 4.11 Yields of the synthesized M-CNPs at different synthesizing temperatures for 5, 7 and 9 wt% of ferrocene to ethanol

4.1.6　Adsorption efficiency (%) of synthesized M-CNPs

In selecting of synthesized M-CNPs to be used as an adsorbent for adsorption antibiotic, the synthesized M-CNPs at condition of 9wt% of ferrocene to ethanol and the synthesizing temperature of 700, 800 and 900°C would be investigated due to the higher carbon yield and for the effect of the crystallinity and the surface area should be studied. In this study was conducted in batch experiments to adsorption of tetracycline (TTC, ≥98% purity, Sigma Aldrich Co.). The wavelength at the maximum absorbance of typical tetracycline solution would be measured by UV-vis Spectrophotometer. The experimental was investigated in the same condition for compare the adsorption efficiency (%) of each various synthesis condition of synthesized M-CNPs that were conducted in flasks containing 250 mL with tetracycline solution of 30 mg/L and initial pH at room temperature with 8.0 mg of synthesized M-CNPs per 25 mL of typical solution. For other details of the absorption would be shown in adsorption experiments.
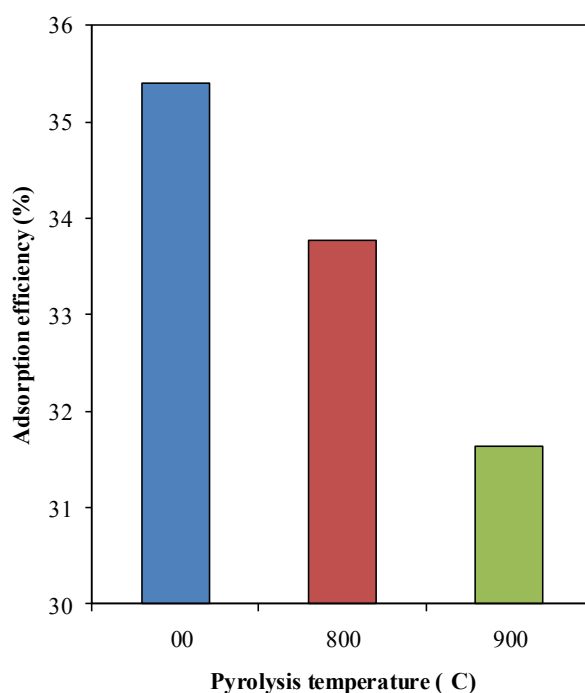
Figure 4.12 Adsorption efficiency (%) of the synthesized M-CNPs at 9wt% of ferrocene to ethanol and 2 L/min of nitrogen gas flow rate at synthesizing temperatures of 700, 800 and 900°C

The percent of adsorption efficiency of synthesized M-CNPs at 9wt% of ferrocene to ethanol at synthesizing temperature of 700, 800 and 900°C that could be indicated when increasing temperature from 700 to 800 and 900°C the adsorption efficiency would be decreased from 35.41 to 33.78 and 31.63, respectively as shown in Figure 4.12. Then the synthesized M-CNPs at 9wt% of ferrocene to ethanol with 700°C of synthesizing temperature were the appropriated condition for adsorption of tetracycline owing to the higher adsorption efficiency with the larger surface area.

4.2   Synthesis of magnetic carbon nanoparticles (M-CNPs) at 9wt% of ferrocene to ethanol with the synthesizing temperature of 700°C

4.2.1   TEM analysis of synthesized M-CNPs morphology

After the SEM analysis, TEM images could be confirmed that the synthesized M-CNPs at 9wt% of ferrocene to ethanol with the synthesizing temperature of 700°C

in Figure 4.13 reveals typical TEM images of the synthesized M-CNPs collected from two different positions along the quartz tube reactor. It could be noticed from Figure 4.11(a) that typical M-CNPs collected from the middle zone of the reactor mainly consists of multi-walled carbon nanotubes (MWCNTs) with nominal diameter about 100 nm. Many iron nanoparticles attached to the tips of such MWCNTs would show an important role in formation of such MWCNTs [24]. Meanwhile, Figure 4.11(b) shows spheroidal carbon nanocapsules (CNCs) containing iron nanoparticles with an average diameter of 60 nm. Such CNCs were mainly collected at the exiting zone of the reactor where the temperature was lower due to the heat radiation effect. An inset shown in Figure 4.11(b) suggests that the carbon nanocapsules are formulated from graphene layers encapsulating the whole surface of iron nanoparticles. Such qualitative evidences would suggest that catalytic iron nanoparticles supplied from ferrocene would be preferably formed as core structures then carbon clusters which were generated from thermal decomposition of ethanol and ferrrocene molecules would be induced to form graphitic layers onto the surface of the iron nanoparticles. It would also note that the local temperature at different location along the reactor axial direction would play an important role in the formation of carbon nanoparticles with different morphologies [24].
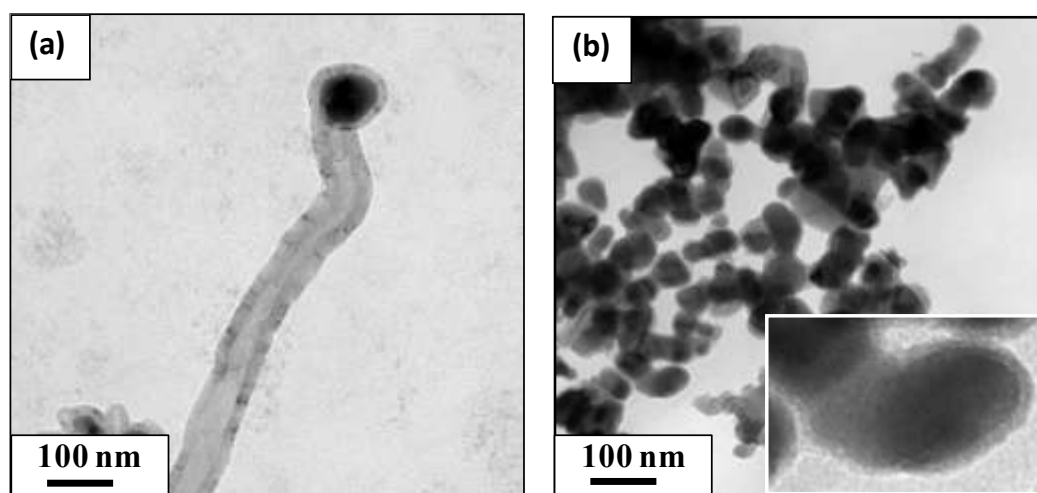
Figure 4.13 TEM images of synthesized products collected from two different positions within the reactor (a) at the middle zone and (b) at the exiting zone

4.2.2 Elemental analysis of the synthesized M-CNPs

4.2.2.1 Energy dispersive X-ray (EDS)

The elemental analysis of synthesized M-CNPs were analysis by the energy dispersive X-ray (EDS) as shown in Figure 4.14. From the result, it could be indicated that the obtained products were composed mainly of carbon (80.66 wt %), O (17.45 wt %) and Fe (1.89 wt %) that could be confirmed the containing of iron particles in the synthesized products.
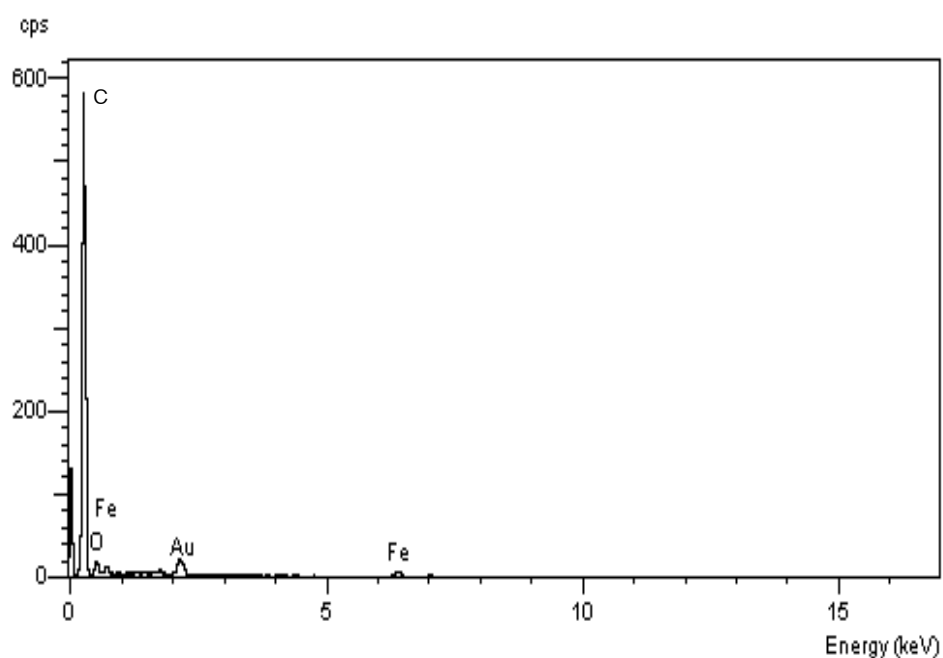
Figure 4.14 EDS spectrum of synthesized M-CNPs at 9wt% of ferrocene to ethanol with synthesizing temperature of $700^{\circ}C$

4.2.2.2 X-ray Diffraction (XRD) analysis

Typical XRD spectra of the synthesized products were shown Figure 4.15. It could be obviously observed that the CNTs with Fe nanoparticles exhibit X-ray diffraction peak at 26.3° which could be specified to the (002) planes of hexagonal graphite [6, 37]. In addition, it can also be observed the existence of Fe with different crystallinities which are the face-centered cubic (fcc) γ-Fe at 43.7° (111) and body-centered cubic (bcc) α-Fe (110) at 44.7°. Moreover, the orthorhombic cementite Fe_3C phase is also seen in the XRD patterns [6]. However, only weak signals could be detected for product samples collected from the entering and exiting zones of the reactors. These results would suggest that the synthesized products collected at the middle zone of the reactor would exhibit the strongest magnetic responses, leading to a higher potential for their applications of magnetic nanomaterials.

From Fe-C phase diagram as presented in Figure 4.16 , it could be described that during the synthesizing temperature was cooling down the γ-Fe (in γ phase and γ + Fe3C phase) were mostly changed into α-Fe because α-Fe is the thermodynamically stable phase at room temperature [38]. This incident was consistent with the appearance of small peak of the γ-Fe in the XRD patterns as shown in Figure 4.13 compared to the α-Fe. While the Fe_3C is not stable at high temperature, then the decomposition of the iron carbide into α-Fe and C atoms was take place, leading to the precipitation of the C atoms to form the CNPs at the surface of the iron particles [39].
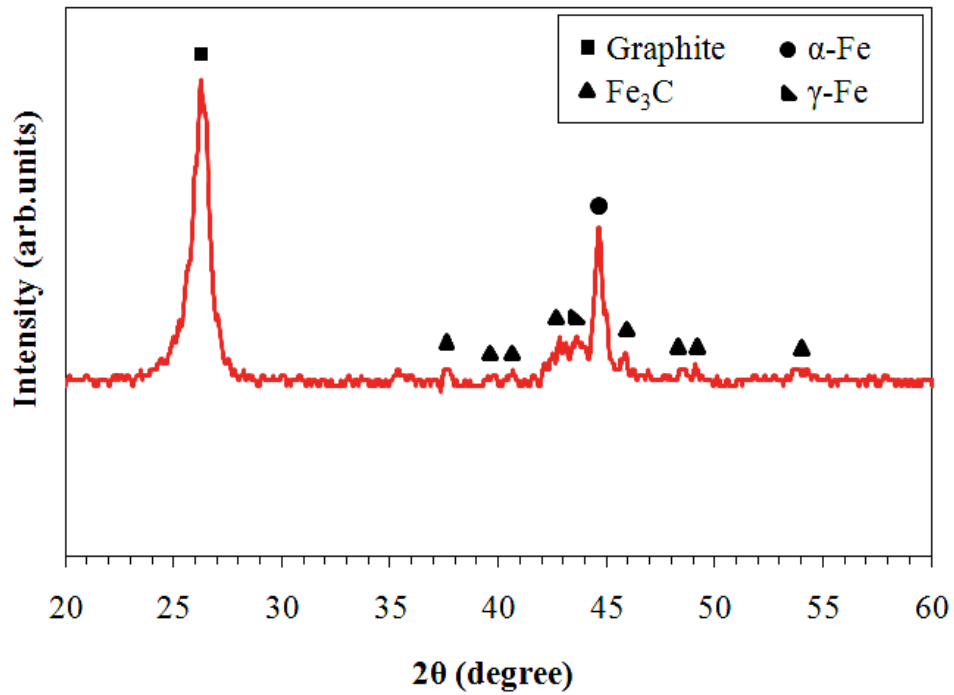
Figure 4.15 XRD patterns of the synthesized M-CNPs at 700°C with 9wt% of ferrocene to ethanol
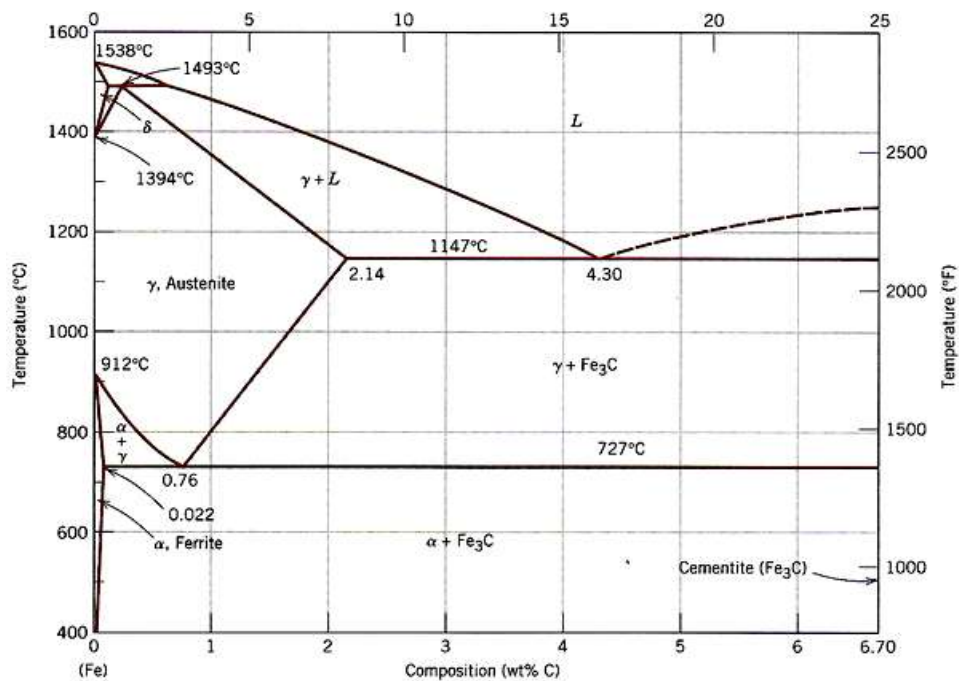
Figure 4.16 the Fe-C Phase Diagram (http://www.chegg.com)

4.2.3   Particle size distribution and zeta potential of synthesized M-CNPs

Particle size distribution of synthesized M-CNPs was analysis by Zetasizer which was shown in Figure 4.17 revealed the radius of synthesized M-CNPs was in a range 50-650 nm which higher than the size from SEM images owing to the agglomeration of the synthesized M-CNPs.
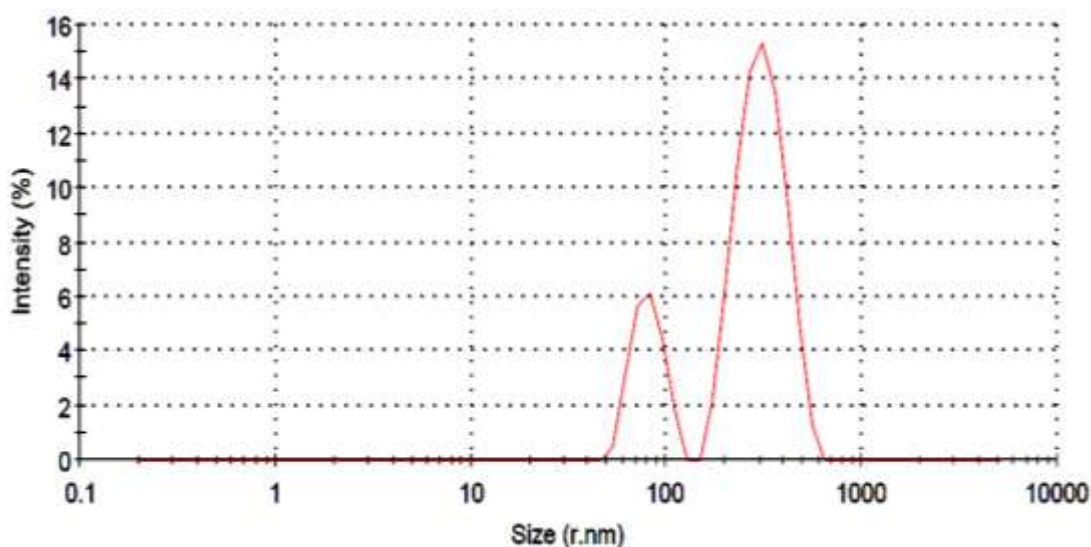
Figure 4.17 Particle size distributions of synthesized M-CNPs at 9wt% of ferrocene to ethanol with the synthesizing temperature of $700^{o}C$

Figure 4.18 depicted the zeta potential of synthesized M-CNPs that was studied about the surface charge. It was indicated that the surface of synthesized M-CNPs was positively charge when the pH value of synthesized M-CNPs solution was below 2.5 and when the pH value of solution was above 2.5 it shown the negatively charge. Then it could be reported that the point of zero charge (pH_{pZC}) of synthesized M-CNPs was at 2.5.
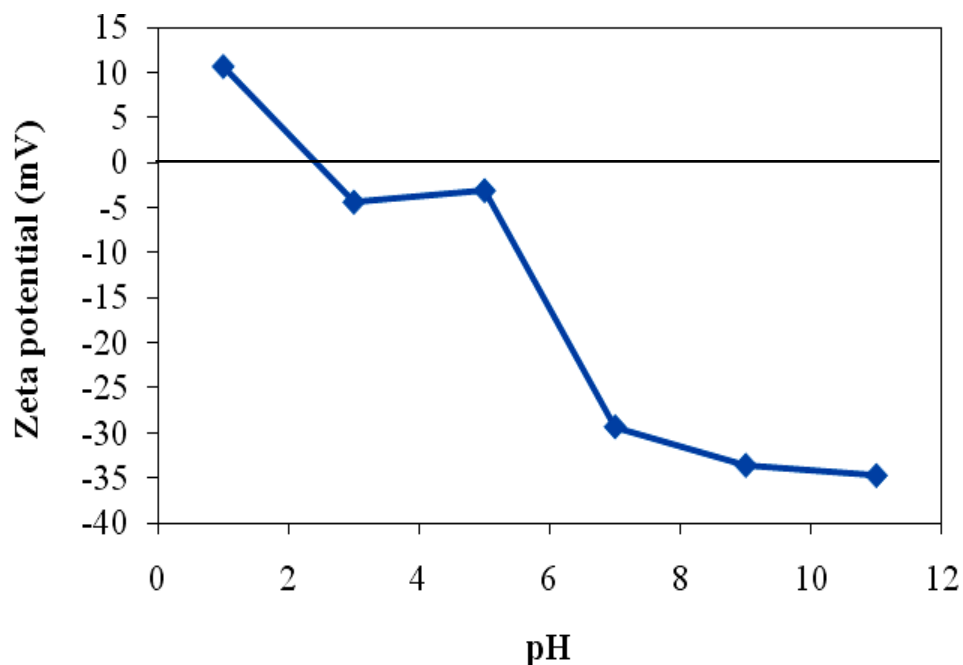
Figure 4.18 Zeta potential of synthesized M-CNPs

4.2.4 BET analysis

The surface area and porosity of synthesized M-CNPs were investigated by BET analyzer under liquid nitrogen temperature (77K). The N_2 adsorption-desorption isotherm as shown in Figure 4.19 could be indicated that the synthesized M-CNPs consisted of two type of porosity micropore and mesopore structure. For specific BET surface area (S_{BET}), total pore volume (V_{tot}) and average pore diameter (D_{avg}) were $47.12 m^2/g$, $0.17 cm^3/g$ and 14.46 nm, respectively.
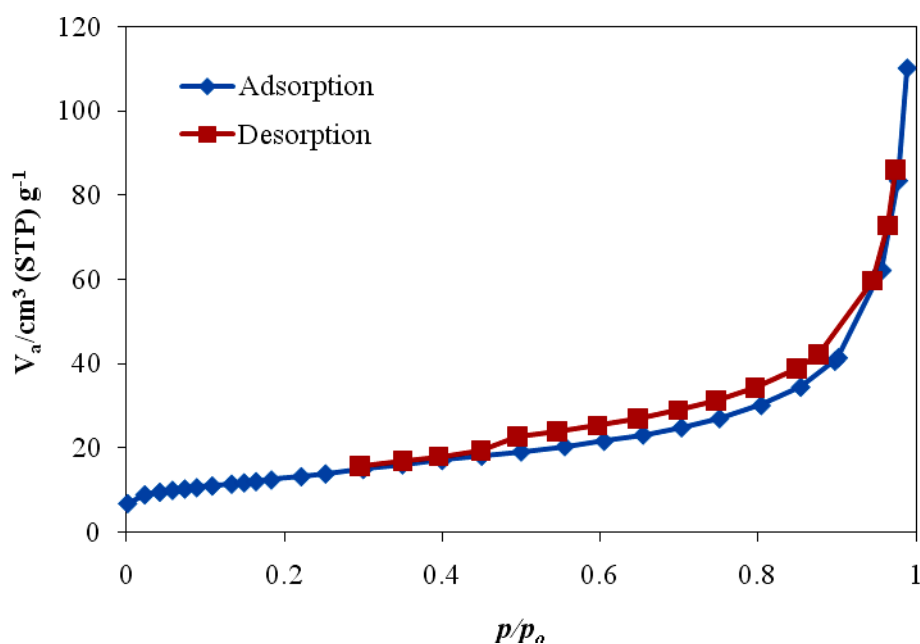
Figure 4.19 N$_2$ adsorption-desorption isotherm of synthesized M-CNPs

4.3   Adsorption experiments

For the adsorption part, the M-CNPs that synthesized at 700oC with 9wt% of ferrocene to ethanol were used as an adsorbent for adsorption antibiotics because it's higher adsorption efficiency (%) when compare with the other condition of synthesized M-CNPs. The tetracycline (≥98% purity, Sigma Aldrich Co.) was utilized as a typical antibiotic for studying the capability in adsorption of M-CNPs. All batch of adsorption experiment were analyzed by using UV-vis spectrophotometer at maximum absorbance wavelength of 357 nm. This parameter that was studied in this research consisted of the contact time, the amount of adsorbent loading, pH value, kinetic modeling and adsorption isotherm. However, the amount of tetracycline adsorbed on M-CNPs and the adsorption efficiency of tetracycline on M-CNPs was calculated by the Equation 4.1 and 4.2.

$$Q_t = \frac{C_0 - C_t}{W} \times V \qquad (4.1)$$

$$Adsorption\ efficiency = \frac{(C_0 - C_t)}{C_0} \times 100 \qquad (4.2)$$

where

Q_t (mg/g)	=	the amount of antibiotics adsorbed per unit mass of M- CNPs at any time
C_0 (mg/L)	=	the initial concentration of antibiotics
C_t (mg/L)	=	the concentration of antibiotics at any time t (min)
V (L)	=	the volume of typical solution
W (g)	=	the mass of the M-CNPs

In this research, the time at equilibrium, the adsorption and desorption rate was equal each other, used to investigated therefore Q_e (mg/g) and C_e (mg/L) were utilized instead of Q_t (mg/g) and C_t (mg/L), respectively.

4.3.1   The amount of M-CNPs loading

The amount of M-CNPs loading for adsorption tetracycline from typical solution was investigated that was a significant parameter to obtain the optimal amount of M-CNPs for using in the other part of adsorption. The amount of M-CNPs in this experiment was studies in the range of 2-12 mg per 25 mL of typical solution. The typical solution was prepared with initial concentration of tetracycline was 30 mg/L in 100 mL after sampling of typical solution at initial time, the M-CNPs was dispersed in the typical solution and was stirred for 600 min to ensure complete equilibrium (the time which reach equilibrium was studied in the contact time part) then the sample was collected again to measure the maximum absorbance by using UV-vis spectrophotometer. The experiment was carried out at 25°C±1 and pH value at 7.0±0.5 (pH of de-ionized water).
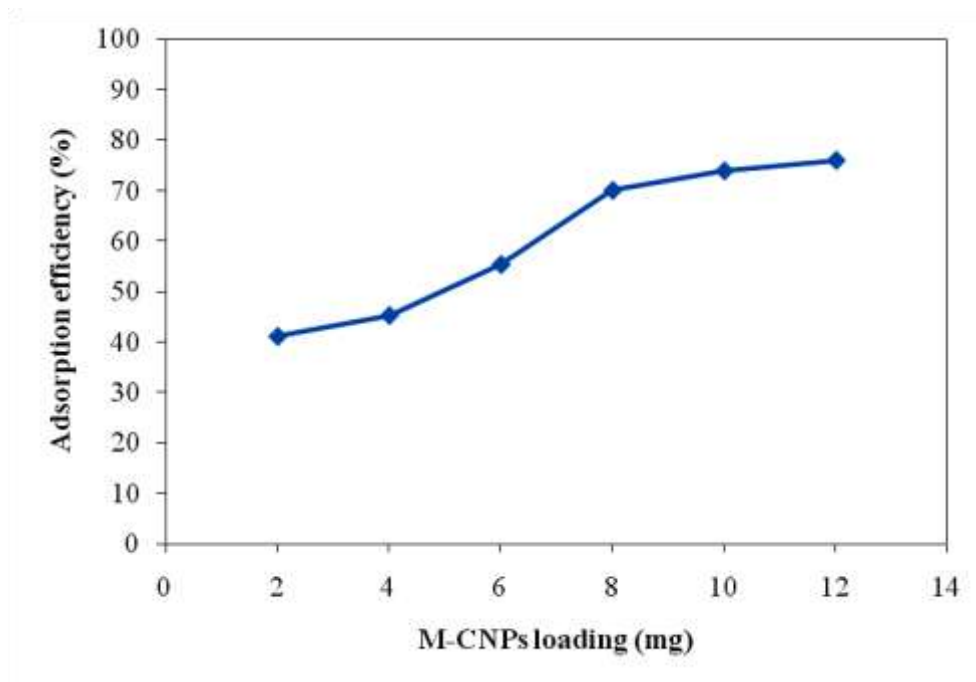
Figure 4.20 Effect of M-CNPs loading on the adsorption of tetracycline on M-CNPs

The plot of the adsorption efficiency versus the amount of M-CNPs loading shown in Figure 4.20 that reveal the adsorption efficiency increased with increasing the amount of M-CNPs until the M-CNPs loading reached 8 mg the increasing of adsorption efficiency shown smaller than the less amount of M-CNPs. It could be suggested that the increasing of the M-CNPs loading would be increased the available active site on surface which leading to increase the adsorption on the surface of M-CNPs. However, even though the increasing of M-CNPs loading would be increased the available active site it also leading to increase the possibility of the agglomeration and entanglement of M-CNPs that inducing to decrease the adsorption on the overlapped external surface of M-CNPs. As the results, it could be indicated that the amount of M-CNPs was started keeping constant at 8.0 mg per 25 mL of typical solution, so this amount would be used in the other part of adsorption experiment.

4.3.2   Effect of initial pH

To studying on effect of initial pH value of typical solution on adsorption by using M-CNPs as an adsorbent was the important parameter. In this research, the initial pH value was investigated in the range of 1-11 with the initial concentration of tetracycline was 30mg/L. The adsorption experiment was carried out on 100 mL of typical solution with the amount of M-CNPs loading was 8 mg per 25 mL (the optimal amount of M-CNPs loading that obtained from the previous investigation) of typical solution. The condition of this experiment was controlled at $25^{\circ}C\pm1$ and adjusted the pH value by 0.1M of NaOH and HCl which was added in the de-ionized water until reaching the require pH value. After sampling at the initial time, the experiment was kept stirring for 600 min to ensure that this experiment reached equilibrium then the sample was collected again to measure the remain of concentration of typical solution.
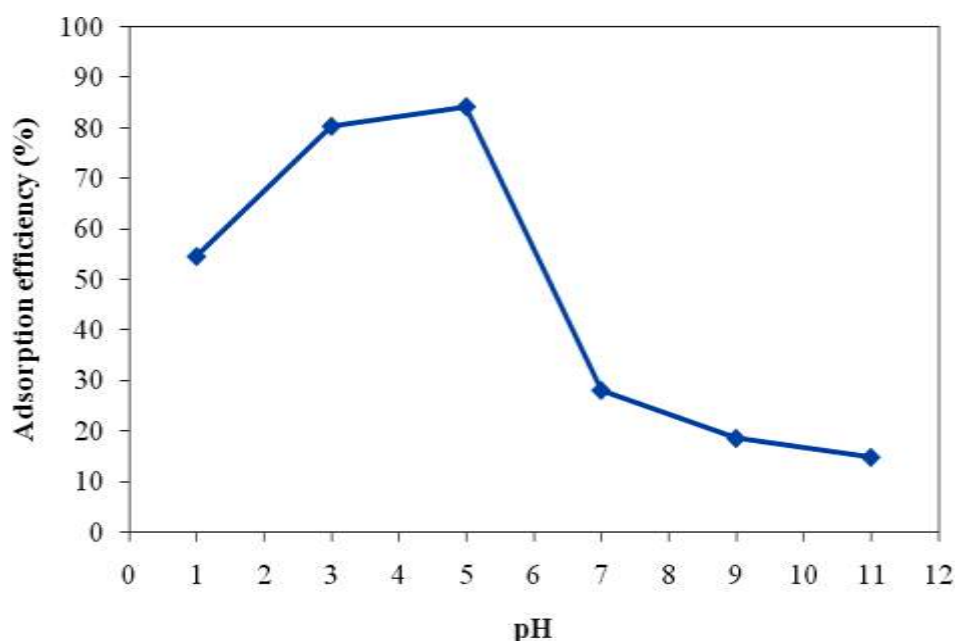
Figure 4.21 Effect of initial pH value on the adsorption of tetracycline on M-CNPs

(a)

(b)
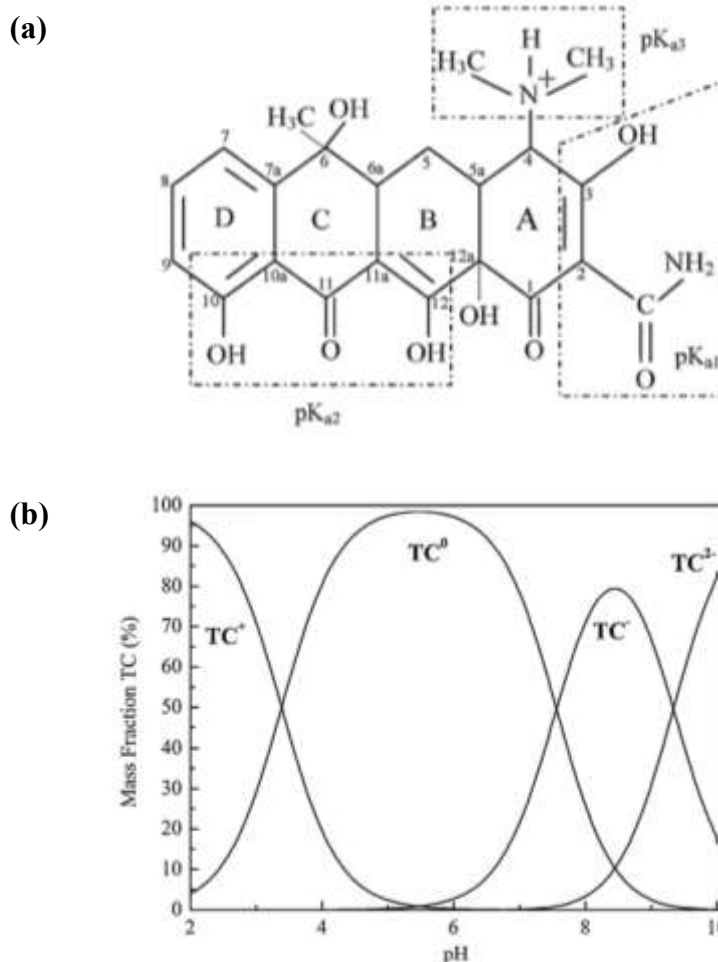
Figure 4.22 Molecular structure of TC (a) and the speciation diagram of TC as a function of pH (b) [40]

The Figure 4.22 revealed the natural of tetracycline would have different charge at different sites based on pH value of solution. At pH below 3.3, tetracycline existed as a cationic form (TCH_3^+) because the dimethyl-ammonium group was protonated. The pH value between 3.3 to 7.7, it existed as zwitterions (TCH_2^0), which predominated and reached a maximum concentration at pH value was 5.0, owing to the loss of proton from the phenolic diketone moiety. When pH value was above 7.7, it was present as anion (TCH^- or TC^{2-}) due to the loss of protons from tricarbonyl

system and phenolic diketone moiety. Therefore, the pK_{a1}, pK_{a2} and pK_{a3} values of tetracycline in aqueous solutions were 3.3, 7.7, and 9.7, respectively [2, 40, 41].

According to the zeta potential result in Figure 4.16 indicated that the point of zero charge (pH_{pZC}) of synthesized M-CNPs was at 2.5so the pH value was below 2.5 shown the positively charge and pH value was above shown the negatively charge.

The Figure 4.21 shown the result of effect of pH value it could be indicated when the pH value from 1 to 5 the percent of adsorption efficiency increased from 54.58 to 84.23 and then decreased until 14. For the pH value increasing from 5 to 11, it could be described by ionization of both the tetracycline and synthesized M-CNPs. The protronation-deprotronation transition of functional group on synthesized M-CNPs would be affected by variation in pH. At pH value of 5 to 11, the adsorption efficiency was decreased due to the influence of electrostatic repulsion between negative charged of tetracycline and synthesized M-CNPs.

4.3.3   Adsorption kinetics

4.3.3.1   Contact time

The Figure 4.23 revealed the adsorption capacity of tetracycline on M-CNPs versus time at different temperature. In this experiment, the temperature was conducted at 25, 45 and 65°C with the initial concentration of tetracycline was 30 mg/L, the pH value of 7.0±0.5 and the amount of M-CNPs loading was 8 mg per 25 mL of typical solution. The sampling was carried out at different time until reaching equilibrium. It could be observed that both adsorption capacity and adsorption rate would significantly be affected by the adsorption temperature. The increasing in the adsorption temperature would result in the increase in both adsorption capacity and rate that higher temperatures leaded to increasing the adsorption capacity from 24.04, 58.93 to 82.81 mg/g when temperature increased from 25, 45 to 65°C. However, the adsorption equilibrium would be achieved within 180 min regardless of adsorption temperature.
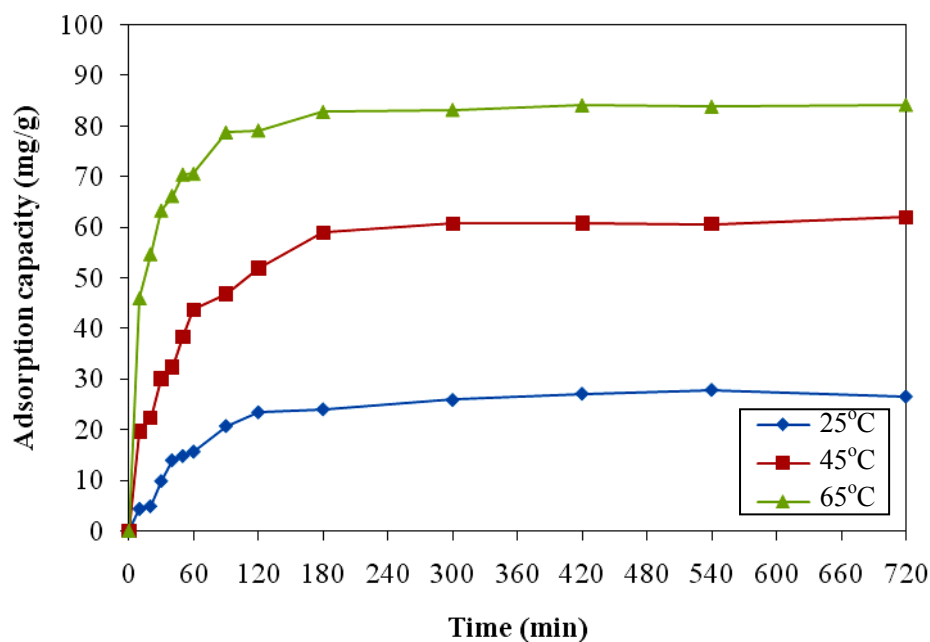
Figure 4.23 Adsorption capacity of tetracycline on M-CNPs versus time at different temperatures

4.3.3.2 Kinetics modeling

For studying the adsorption process of tetracycline on synthesized M-CNPs , the kinetics models including the pseudo-first-order and pseudo-second-order models was used to investigate.

Pseudo-first-order model

The Equation 4.3 was used to describe the pseudo-first-order as shown below, after integrating it for the boundary condition $t=0$ to $t=t$ and $Q_t=0$ to $Q_t=Q_t$, it could be rearranged for linearized data plots that shown in Equation 4.4.

$$\frac{dQ_e}{dt} = k_1(Q_e - Q_t) \tag{4.3}$$

$$\log(Q_e - Q_t) = \log(Q_e) - \frac{k_1 t}{2.303} \tag{4.4}$$

where

Q_e (mg/g)	=	the amount of tetracycline adsorbed onto synthesized M-CNPs at equilibrium
Q_t (mg/g)	=	the amount of tetracycline adsorbed onto synthesized M-CNPs at time t (min)
k_1 (min^{-1})	=	the rate constant of the pseudo-first-order adsorption

The values k_1 could be determined by plot of ln $(Q_e$-$Q_t)$ versus t.

Pseudo-second-order model

The Equation 4.5 was used to study the pseudo-first order kinetic model. Integrating this equation for boundary condition t=0 to t=t and Q_t=0 to Q_t=Q_t, it could be rearranged for linearized data plots that shown in Equation 4.6.

$$\frac{dQ_e}{dt} = k_2(Q_e - Q_t)^2 \tag{4.5}$$

$$\frac{t}{Q_t} = \frac{1}{k_2 Q_e^2} + \frac{1}{Q_e} t \tag{4.6}$$

where

k_2 (g/mg-min) = the second-order rate constant that obtained by plot of t/Q_t versus t

The initial adsorption rate h (mg/g-min) could be determined from Equation 4.7.

$$h = k_2 Q_e^2 \tag{4.7}$$

For the result from Figure 4.24 and 4.25 indicated that the adsorption kinetics suited to fit with both of the pseudo-first-order and the pseudo-second-order models that could be describe by the value of R^2. The experimental data of the kinetic parameters including of the initial sorption rate values were lists in Table 4.1 for pseudo-first-order and Table 4.2 for pseudo-second-order.

According to the experimental data of adsorption kinetics based on the correlation coefficients, the adsorption of tetracycline was better described by the pseudo-second-order model. Not only the value of R^2 nearly 1 but the amount of tetracycline adsorbed onto synthesized M-CNPs at equilibrium which determined by experiment ($Q_{e,Exp}$) and by calculation ($Q_{e,Cal}$) was got closer together when compare with the pseudo-first-order model. However, the initial adsorption rate, h (mg/g-min), increased when the temperature was increased to give adsorption system.

Table 4.1 Kinetic parameters of pseudo-first-order for tetracycline adsorption on synthesized M-CNPs at different temperatures

T(°C)	Pseudo-first-order model			
	$Q_{e,Exp}$ (mg/g)	$Q_{e,Cal}$ (mg/g)	k_1 (min^{-1})	R^2
25	24.04	24.53	0.0214	0.8735
45	58.93	57.65	0.0207	0.9685
65	82.81	46.26	0.0226	0.9547

Table 4.2 Kinetic parameters of pseudo-second-order for tetracycline adsorption on synthesized M-CNPs at different temperatures

T(^{o}C)	Pseudo-second-order model				
	$Q_{e,Exp}$ (mg/g)	$Q_{e,Cal}$ (mg/g)	k_2 (min^{-1})	h (mg/g-min)	R^2
25	24.04	32.05	0.0005	0.5612	0.8048
45	58.93	64.52	0.0006	2.3240	0.9564
65	82.81	85.47	0.0013	9.5877	0.9956
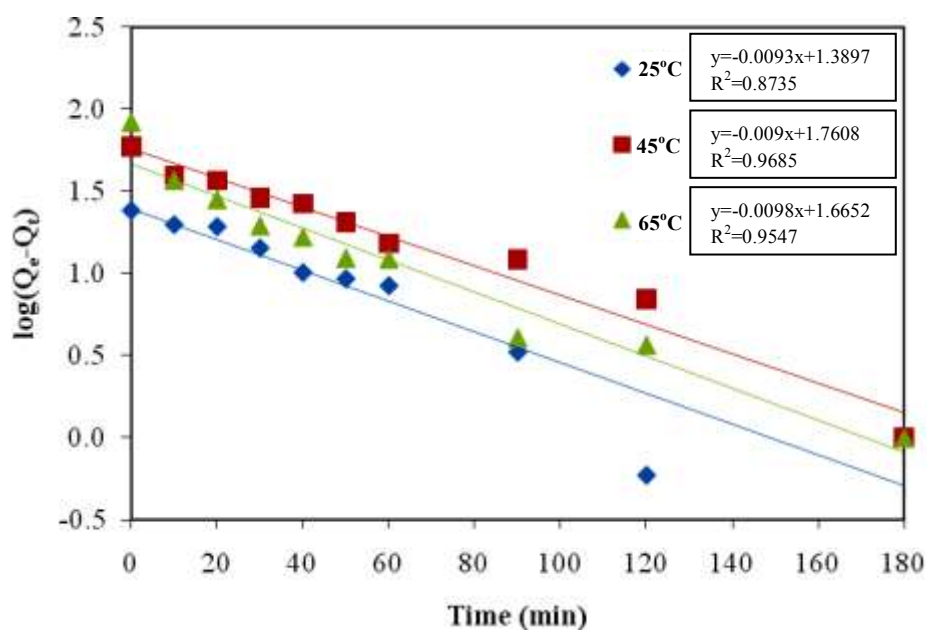
Figure 4.24 Pseudo-first-order plots for the adsorption of tetracycline onto synthesized M-CNPs at different temperature
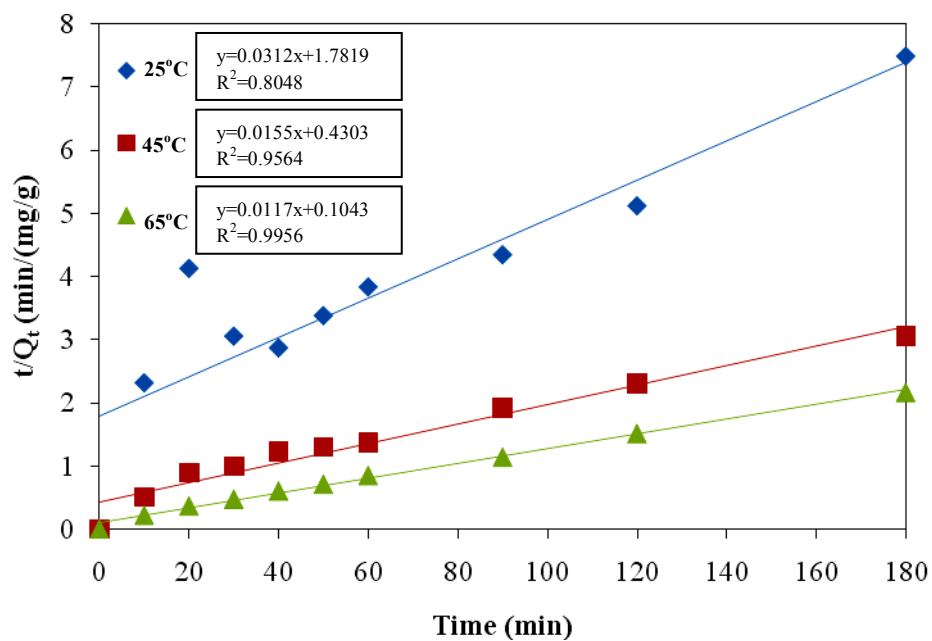
Figure 4.25 Pseudo-second-order plots for the adsorption of tetracycline onto synthesized M-CNPs at different temperature

The energy of adsorption (E_a) for the adsorption could be described by using Arrhenius equation based on the got k_2 values in Table 4.2 as revealed in Equation 4.8.

$$k = Ae\left(\frac{-E_a}{RT}\right)$$ (4.8)

where

A (min-1)	=	the frequency factor
E_a (kJ/mol)	=	the energy of adsorption
R (J/mol-K)	=	the ideal gas constant
T (K)	=	the absolute temperature (K)

When taking logarithm on Equation 4.8, it could be converted into Equation 4.9 as shown below:

$$\ln k_2 = \ln A - \frac{E_a}{RT} \qquad (4.9)$$
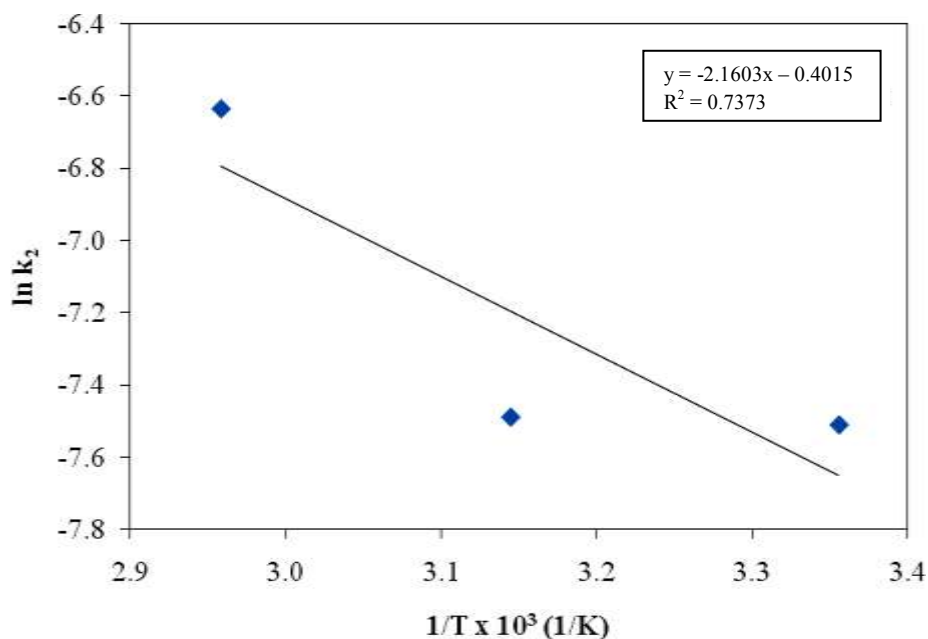
Figure 4.26 Correlation between ln k_2 and 1000/T of tetracycline adsorbed onto synthesized M-CNPs

Therefore, E_a could be obtained from the slope of the line plotting ln k_2 against 1000/T as revealed in Figure 4.26. The value of determined E_a for tetracycline adsorption on synthesized M-CNPs was 17.96kJ/mol. The E_a value could be indicated that the lower of E_a leaded to the less sensitive of temperature affected on the adsorption reaction and shown the process could be easily conducted.

4.3.4   Adsorption isotherms

The adsorption isotherm for tetracycline that described how tetracycline interacted with synthesized M-CNPs. The adsorption experiment was conducted at initial tetracycline concentration range of 10-100 mg/L with different temperature of 25, 45 and 65°C as shown in Figure 4.27. The adsorption amount of tetracycline onto synthesized M-CNPs at equilibrium as a function of the initial tetracycline concentration at equilibrium was investigated. The experiment data was also analyzed with Langmuir and Freundlich isotherm model following Equation 2.1 and 2.3, respectively. For Langmuir isotherm model was conducted by plotting C_e/Q_e versus C_e as revealed in Figure 4.28 and plotting log Q_e versus log C_e for Freundlich isotherm model as shown in Figure 4.29. However, the constant values of Langmuir and Freundlich isotherm model were shown in Table 4.3.

From Table 4.3, the correlation coefficients (R^2) of adsorption tetracycline on synthesized M-CNPs of Freundlich isotherm showed higher than Langmuir isotherm under the studied concentration range. Therefore, the Freundlich isotherm fitted better compared with the Langmuir isotherm in all condition. However, the maximum adsorption capacity of tetracycline onto synthesized M-CNPs was 211.35, 231.39 and 285.18 mg/g when increased the temperature from 25, 45 to 65°C, respectively [5.9]. The lower of Langmuir constant value (K_L) showed the weaker attraction toward the site of CNPs charge. For the necessary feature of the Langmuir isotherm could be expressed by R_L that found between zero and unity, indicated that adsorption was more favorable for higher initial concentration of tetracycline. For $1/n = 1$, indicating that the adsorption is constant (independent of the solute solution), but for $1/n < 1$, the adsorption strength decrease when the concentration of solution increased [5.7].
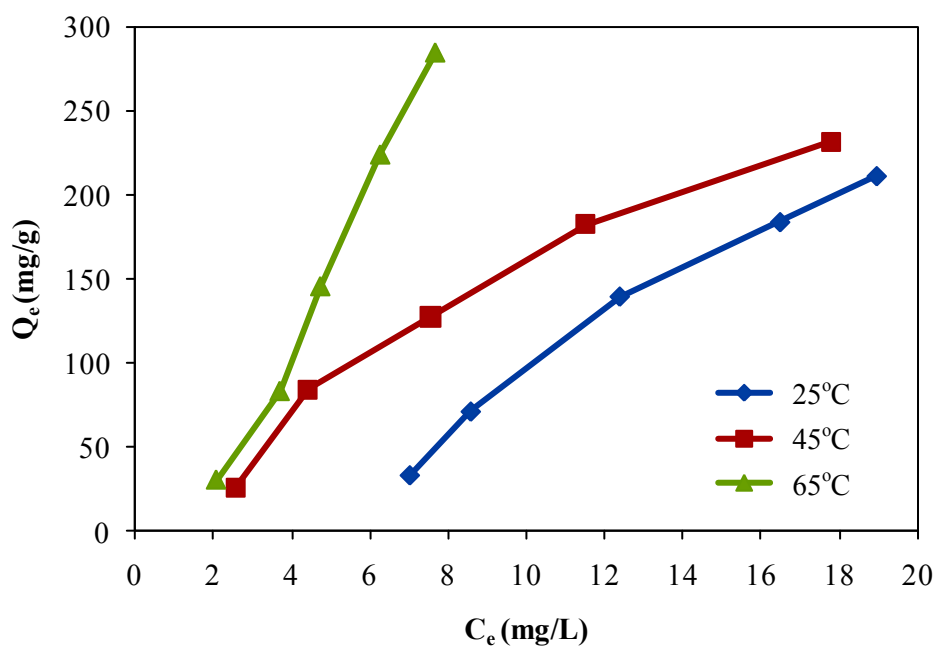
Figure 4.27 Adsorption isotherm of tetracycline at different temperature and the initial tetracycline concentration was in the range of 10-100 mg/L
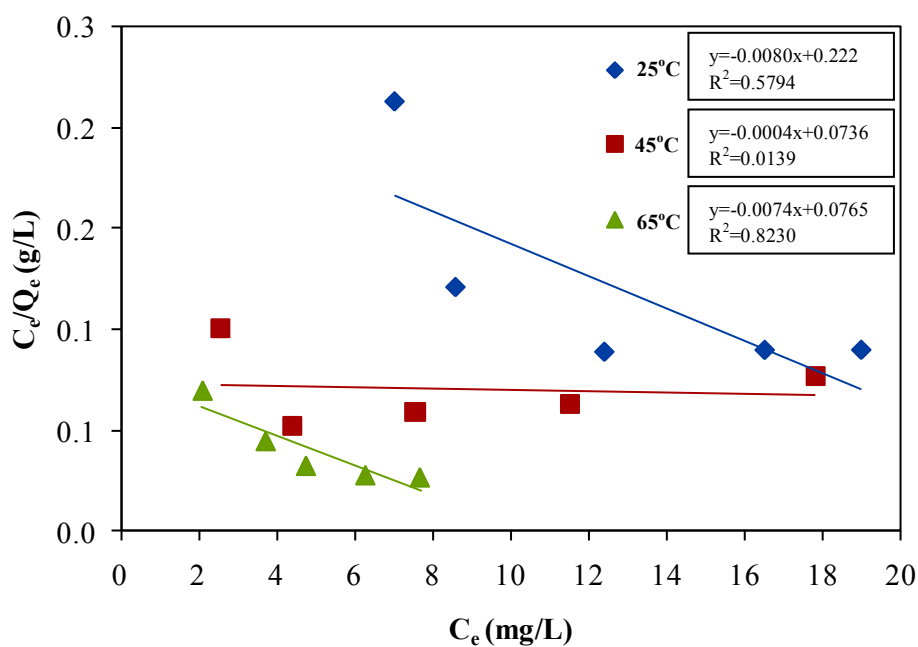
Figure 4.28 Langmuir isotherm plots for the adsorption of tetracycline at different temperature and the initial tetracycline concentration was in the range of 10-100 mg/L
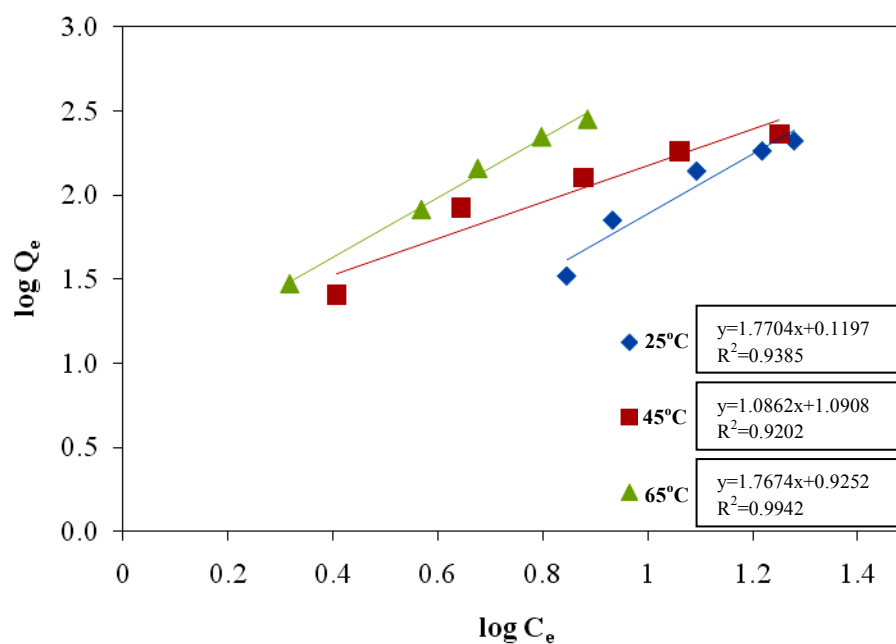
Figure 4.29 Freundlich isotherm plots for the adsorption of tetracycline at different temperature and the initial tetracycline concentration was in the range of 10-100 mg/L

Table 4.3 The constant value of Langmuir and Freundlich isotherms for the adsorption of tetracycline at different temperature

T (^{o}C)	Langmuir model				Freundlich model		
	Q_m (mg/g)	K_L (L/mg)	R_L	R^2	K_F (mg/g)(L/mg)^n	n	R^2
25	211.35	0.0213	0.3427-0.8243	0.5794	1.3173	0.5648	0.9385
45	231.39	0.0587	0.1591-0.6300	0.0139	12.3254	0.9206	0.9202
65	285.18	0.0458	0.1951-0.6857	0.8230	8.4178	0.5658	0.9942

4.4   Separation efficiency (%) of synthesized M-CNPs after adsorption by external permanent magnet

For adsorption characteristics of tetracycline onto synthesized M-CNPs as shown in Figure 4.30 (a) was the typical solution of tetracycline (the left bottle) and the suspension of synthesized M-CNPs in typical solution and Figure 4.30 (b) played the typical solution of tetracycline (the left bottle) and separation of synthesized M-CNPs from typical solution by external permanent magnet. The magnetic property of such synthesized M-CNPs could provide a possibility for their collection using external permanent magnet which would help reduce difficulty in their handling.

The synthesized M-CNPs after adsorption were separated from typical solution and were dried at 100°C for overnight. After that the dried M-CNPs were weighed to measure the weight loss of synthesized M-CNPs that could not be separated by external permanent magnet by using Equation 4.10.

$$Weight\ loss\ (\%) = \frac{initial\ weight\ -\ final\ weight}{initial\ weight} \times 100 \qquad (4.10)$$

For the result, the weight loss of synthesized M-CNPs was only 4.88% that could not be separated by external permanent magnet. So, it could be determined the synthesized M-CNPs could be separated from typical solution by external permanent magnet was about 95.12%.
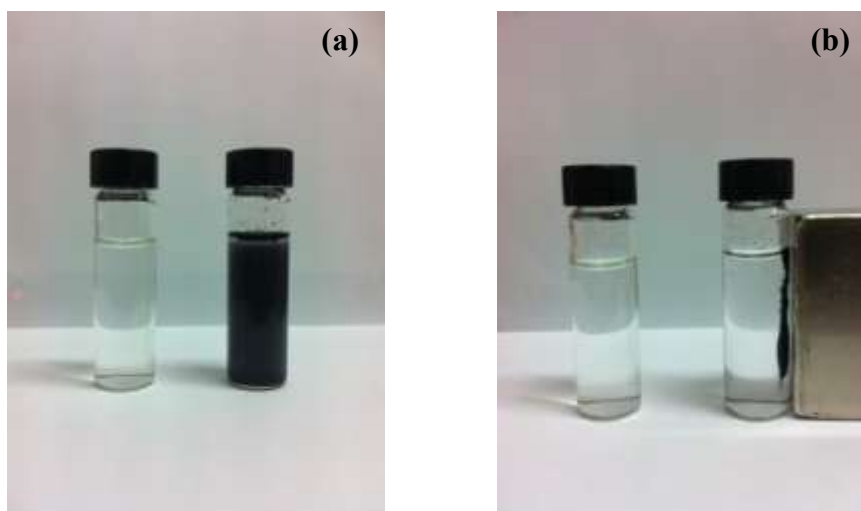
Figure 4.30 The photographs of synthesized M-CNPs adsorption behavior with the external permanent magnet (a) the typical solution of tetracycline and the suspension of synthesized M-CNPs in typical solution and (b) the typical solution of tetracycline and separation of synthesized M-CNPs from typical solution by external permanent magnet

CHAPTER V

CONCLUSION AND RECOMMENDATION

5.1   Conclusions

5.1.1   Synthesis of Magnetic carbon nanoparticles (M-CNPs) by co-pyrolysis of ethanol and ferrocene

In this work, M-CNPs could be synthesized using co-pyrolysis of ethanol with the presence of ferrrocene. It was found that the condition appropriate for synthesis of M-CNPs is to co-pyrolyse ethanol with 9 wt% of ferrocene at 700 ^{o}C. Typically, the synthesized M-CNPs consist of two distinctive morphological characteristics, carbon nanotubes with diameter of 100 nm and carbon nanocapsules with diameter of 60 nm. Main product could be collected at the middle zone of the quartz tube reactor. In addition I_D/I_G ratio Raman spectrum of the synthesized M-CNPs reveals they contain a higher content of graphitic carbon nanostructure than that of amorphous carbon. The iron nanoparticles in synthesized M-CNPs were consisted of austenite (γ-Fe), ferrite (α-Fe) and iron carbide (Fe_3C) by analyze with XRD analysis. For specific BET surface area (S_{BET}), total pore volume (V_{tot}) and average pore diameter (D_{avg}) were 47.12m^2/g, 0.17cm^3/g and 14.46 nm, respectively which could be identified as micropore and mesopore. According to the result of analysis and magnetic property of synthesized M-CNPs, it could be leaded to use as an adsorbent of application in adsorption of tetracycline.

5.1.2 Adsorption of tetracycline by using synthesized M-CNPs

For adsorption studies, the adsorption behavior of tetracycline onto synthesized M-CNPs was investigated. The optimal amount of synthesized M-CNPs loading in typical solution was 8.0 mg per 25 mL of typical solution and at pH value of 5 showed the highest adsorption efficiency of 84.23%. The result of adsorption kinetics, it indicated that increasing temperature will result to adsorption capacity increase from 24.04, 58.93 to 82.81 mg/g when temperature increased from 25, 45 to $65^{o}C$. For the effect of contact time, the adsorption would reach equilibrium within 180 min. The kinetic model was better fitted by pseudo-second-order and Freundlich model for adsorption isotherm.

Such M-CNPs were suitable to be applied as an adsorbent for removal of antibiotic contaminating in simulated wastewater. It should be noted that magnetic properties is a unique characteristic which is essential for a separation process using a simple magnetic process which the separation efficiency (%) of synthesized M-CNPs after adsorption by external permanent magnet as high as 95.12%.

5.2 Recommendation for Future Work

According to the result of experiment, it revealed that synthesized M-CNPs could be applied as an adsorbent for removal tetracycline from typical solution by emphasis in the field of magnetic property. Therefore, the magnetism of the synthesized M-CNPs should be investigated. However, the desorption of tetracycline from synthesized M-CNPs was the interesting point for reuse the synthesized M-CNPs again including the adsorption process should be improved and designed for large scale production.

REFERENCES

[1]   Kay, P., P.A. Blackwell, and A.B. Boxall. A lysimeter experiment to investigate the leaching of veterinary antibiotics through a clay soil and comparison with field data. <u>Environ Pollut</u>, 134, 2 (2005): 333-41.

[2]   Zhang, L., et al. Studies on the removal of tetracycline by multi-walled carbon nanotubes. <u>Chemical Engineering Journal</u>, 178, (2011): 26-33.

[3]   Zhang, W., et al. A comparative study of the adsorption properties of 1-naphthylamine by XAD-4 and NDA-150 polymer resins. <u>Colloids and Surfaces A: Physicochemical and Engineering Aspects</u>, 331, 3 (2008): 257-262.

[4]   Crini, G. Non-conventional low-cost adsorbents for dye removal: A review. <u>Bioresource Technology</u>, 97, 9 (2006): 1061-1085.

[5]   Gong, J.L., et al. Removal of cationic dyes from aqueous solution using magnetic multi-wall carbon nanotube nanocomposite as adsorbent. <u>J Hazard Mater</u>, 164, 2-3 (2009): 1517-22.

[6]   Liu, Q., et al. Synthesis of different magnetic carbon nanostructures by the pyrolysis of ferrocene at different sublimation temperatures. <u>Carbon</u>, 46, 14 (2008): 1892-1902.

[7]   Ren, X., et al. Carbon nanotubes as adsorbents in environmental pollution management: A review. <u>Chemical Engineering Journal</u>, 170, 2-3 (2011): 395-410.

[8]   Ai, L., et al. Removal of methylene blue from aqueous solution with magnetite loaded multi-wall carbon nanotube: Kinetic, isotherm and mechanism analysis. <u>Journal of Hazardous Materials</u>, 198, (2011): 282-290.

[9]   Qu, S., et al. Magnetic removal of dyes from aqueous solution using multi-walled carbon nanotubes filled with Fe_2O_3 particles. <u>Journal of Hazardous Materials</u>, 160, 2-3 (2008): 643-647.

[10] Joseph, L., et al. Adsorption of bisphenol A and 1 α -ethinyl estradiol on single walled carbon nanotubes from seawater and brackish water. <u>Desalination</u>, 281, (2011): 68-74.

[11] Joseph, L., et al. Removal of bisphenol A and 1 α -ethinyl estradiol from landfill leachate using single-walled carbon nanotubes. <u>Water Research</u>, 45, 13 (2011): 4056-4068.

[12] Darabont, A., et al. Synthesis of carbon nanotubes by spray pyrolysis and their investigation by electron microscopy. <u>Journal of Optoelectronics and Advanced Materials</u>, 7, 2 (2005): 631-636.

[13] Lupo, F., et al. Pyrolytic synthesis of long strands of large diameter single-walled carbon nanotubes at atmospheric pressure in the absence of sulphur and hydrogen. <u>Chemical Physics Letters</u>, 410, 4-6 (2005): 384-390.

[14] Kroto, H.W., et al. C60: Buckminsterfullerene. <u>Nature</u>, 318, 6042 (1985): 162-163.

[15] Iijima, S. Helical microtubules of graphitic carbon. <u>Nature</u>, 354, 6348 (1991): 56-58.

[16] T. Guo, P.N., A. Thess, D.T. Colbert, R.E. Smalley. Catalytic growth of single-walled nanotubes by laser vaporization. <u>Chemical Physics Letters</u>, 243 (1995): 49-54.

[17] Muhammad Musaddique Ali Rafique*, J.I. Production of Carbon Nanotubes by Different Routes— A Review. <u>Journal of Encapsulation and Adsorption Sciences</u>, 1, (2011): 29-34.

[18] Thiele-Bruhn, S. Pharmaceutical antibiotic compound in soils - a review. <u>J. Plant Nutr. Soil Sci.</u>, 166, (2003): 145-167.

[19] Grassi, G.G. Tetracyclines - extending the atypical spectrum. <u>International Journal ofAntimicrobial Agents</u>, 3, (1993): S31-S46.

[20] Langmuir, I. The adsorption of gases on plane surfaces of glass, mica and platinum. <u>The research laboratory of general electric company</u>, (1918): 1361-1403.

[21] Lee, Y.T., et al. Temperature-dependent growth of carbon nanotubes by pyrolysis of ferrocene and acetylene in the range between 700 and 1000 °C. <u>Chemical Physics Letters</u>, 372, 5-6 (2003): 853-859.

[22] Sano, N. and M. Uehara. Selective formation of Fe-included carbon nanocapsules and nanotubes by fall-to-stop pyrolysis reactor with

ferrocene. <u>Chemical Engineering and Processing: Process Intensification</u>, 45, 7 (2006): 555-558.

[23] Chaisitsak, S., J. Nukeaw, and A. Tuantranont. Parametric study of atmospheric-pressure single-walled carbon nanotubes growth by ferrocene–ethanol mist CVD. <u>Diamond and Related Materials</u>, 16, 11 (2007): 1958-1966.

[24] Charinpanitkul, T., et al. Naphthalene as an alternative carbon source for pyrolytic synthesis of carbon nanostructures. <u>Journal of Analytical and Applied Pyrolysis</u>, 86, 2 (2009): 386-390.

[25] Zhao, Q., et al. Synthesis of multi-wall carbon nanotubes by the pyrolysis of ethanol on Fe/MCM-41 mesoporous molecular sieves. <u>Superlattices and Microstructures</u>, 47, 3 (2010): 432-441.

[26] Qu, S., et al. Magnetic removal of dyes from aqueous solution using multi-walled carbon nanotubes filled with Fe_2O_3 particles. <u>J Hazard Mater</u>, 160, 2-3 (2008): 643-7.

[27] Tang, W.-W., et al. Simultaneous adsorption of atrazine and Cu (II) from wastewater by magnetic multi-walled carbon nanotube. <u>Chemical Engineering Journal</u>, 211-212, (2012): 470-478.

[28] Maryam Jafari, S.F., Aghamiri and Gholamreza Khaghanic. Batch Adsorption of Cephalosporins Antibiotics from Aqueous Solution by Means of Multi-Walled Carbon Nanotubes. <u>World Applied Sciences Journal</u>, 14, 11 (2011): 1642-1650.

[29] Zhang, L., et al. Adsorption behavior of multi-walled carbon nanotubes for the removal of olaquindox from aqueous solutions. <u>Journal of Hazardous Materials</u>, 197, (2011): 389-396.

[30] Carabineiro, S.A.C., et al. Comparison between activated carbon, carbon xerogel and carbon nanotubes for the adsorption of the antibiotic ciprofloxacin. <u>Catalysis Today</u>, 186, 1 (2012): 29-34.

[31] Zhang, D., et al. Adsorption of sulfamethoxazole on functionalized carbon nanotubes as affected by cations and anions. <u>Environ Pollut</u>, 159, 10 (2011): 2616-21.

[32] Puengjinda, P., et al. Selective synthesis of carbon nanotubes and nanocapsules using naphthalene pyrolysis assisted with ferrocene. <u>Journal of Industrial and Engineering Chemistry</u>, 15, 3 (2009): 375-380.

[33] Zhang, H., et al. Layered growth of aligned carbon nanotube arrays by pyrolysis. <u>Physica B: Condensed Matter</u>, 337, 1-4 (2003): 10-16.

[34] Sano, N., et al. Separated synthesis of iron-included carbon nanocapsules and nanotubes by pyrolysis of ferrocene in pure hydrogen. <u>Carbon</u>, 41, 11 (2003): 2159-2162.

[35] Kanchan Samant, S.K.H., and Sudhir Kapoor. Synthesis of carbon nanotubes by catalytic vapor decomposition (CVD) method: Optimization of various parameters for the maximum yield. <u>journal of physics</u>, 68, 1 (2007): 51–60.

[36] Park, Y.T.L.a.J. Temperature-Dependent Growth of Vertically Aligned Carbon Nanotubes in the Range 800-1100 °C. <u>J. Phys. Chem. B</u>, 106, (2002): 7614-7618.

[37] Wang, H., et al. An efficient method for decoration of the multiwalled carbon nanotubes with nearly monodispersed magnetite nanoparticles. <u>Materials Science and Engineering: B</u>, 164, 3 (2009): 191-194.

[38] Cheng, J., et al. Synthesis of iron-filled carbon nanotubes with a great excess of ferrocene and their magnetic properties. <u>Solid State Communications</u>, 149, 39-40 (2009): 1619-1622.

[39] J.-W. Snoeck, G.F.F., and M. Fowlesz. Filamentous Carbon Formation and Gasification: Thermodynamics, Driving Force, Nucleation, and Steady-State Growth. <u>JOURNAL OF CATALYSIS</u>, 169, (1997): 240–249.

[40] Liu, N., et al. Sorption of tetracycline on organo-montmorillonites. <u>J Hazard Mater</u>, 225-226, (2012): 28-35.

[41] Chang, P.-H., et al. Adsorption and intercalation of tetracycline by swelling clay minerals. <u>Applied Clay Science</u>, 46, 1 (2009): 27-36.

APPENDICES

APPENDIX A

STANDARD CURVE OF TETRACYCLINE

Table A.1 The initial concentration and the absorbance of tetracycline at λ_{max} =357 nm

Concentration (mg/L)	Absorbance
10	0.2907
20	0.5770
30	0.8973
40	1.2230
50	1.5283
60	1.8773
70	2.1983
80	2.5520
90	2.8207
100	3.0870
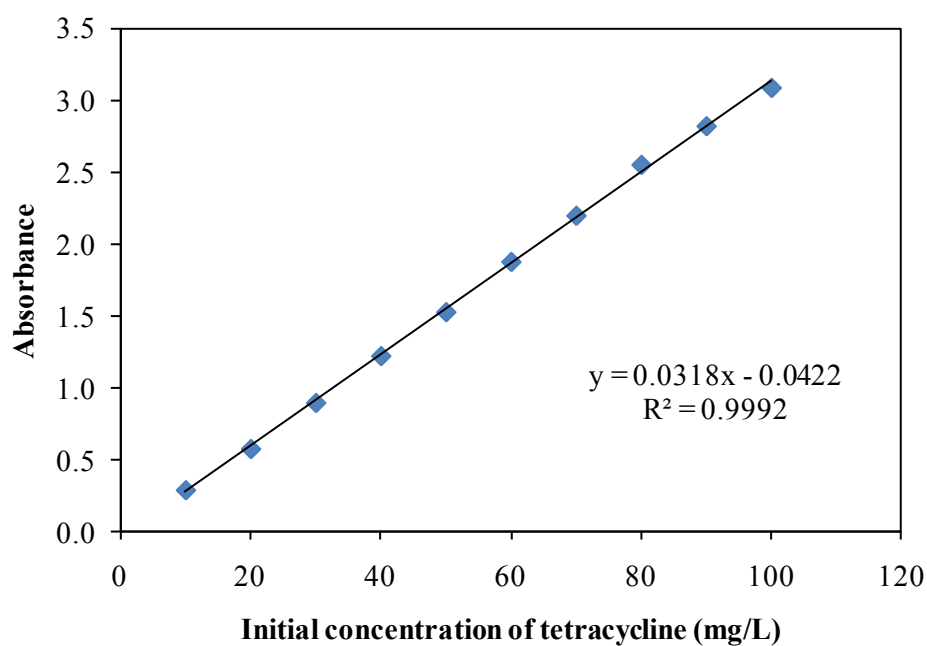
Figure A.1 Standard curve of tetracycline at λ_{max} = 357 nm

APPENDIX B

ADSORPTION ISOTHERM

Table B.1 Langmuir adsorption isotherm of tetracycline at 25°C

Initial concentration (mg/L)	Equilibrium concentration (C_e) (mg/L)	Equilibrium adsorption capacity (Q_e) (mg/g)	C_e/Q_e (g/L)
10	7.019	32.986	0.213
30	8.581	70.984	0.121
50	12.396	139.544	0.089
70	16.505	183.930	0.090
90	18.979	211.347	0.090

Table B.2 Langmuir adsorption isotherm of tetracycline at 45°C

Initial concentration (mg/L)	Equilibrium concentration (C_e) (mg/L)	Equilibrium adsorption capacity (Q_e) (mg/g)	C_e/Q_e (g/L)
10	2.553	25.452	0.100
30	4.409	84.185	0.052
50	7.543	127.227	0.059
70	11.516	182.226	0.063
90	17.805	231.394	0.077

Table B.3 Langmuir adsorption isotherm of tetracycline at 65°C

Initial concentration (mg/L)	Equilibrium concentration (C_e) (mg/L)	Equilibrium adsorption capacity (Q_e) (mg/g)	C_e/Q_e (g/L)
10	2.082	29.972	0.069
30	3.706	82.875	0.045
50	4.744	145.506	0.033
70	6.275	224.220	0.028
90	7.679	285.181	0.027

Table B.4 Freundlich adsorption isotherm of tetracycline at 25°C

Initial concentration (mg/L)	Equilibrium concentration (C_e) (mg/L)	Equilibrium adsorption capacity (Q_e) (mg/g)	log C_e	log Q_e
10	7.019	32.986	0.846	1.518
30	8.581	70.984	0.934	1.851
50	12.396	139.544	1.093	2.145
70	16.505	183.930	1.218	2.265
90	18.979	211.347	1.278	2.325

Table B.5 Freundlich adsorption isotherm of tetracycline at 45°C

Initial concentration (mg/L)	Equilibrium concentration (C_e) (mg/L)	Equilibrium adsorption capacity (Q_e) (mg/g)	log C_e	log Q_e
10	2.553	25.452	0.407	1.406
30	4.409	84.185	0.644	1.925
50	7.543	127.227	0.878	2.105
70	11.516	182.226	1.061	2.261
90	17.805	231.394	1.251	2.364

Table B.6 Freundlich adsorption isotherm of tetracycline at 65°C

Initial concentration (mg/L)	Equilibrium concentration (C_e) (mg/L)	Equilibrium adsorption capacity (Q_e) (mg/g)	log C_e	log Q_e
10	2.082	29.972	0.318	1.477
30	3.706	82.875	0.569	1.918
50	4.744	145.506	0.676	2.163
70	6.275	224.220	0.798	2.351
90	7.679	285.181	0.885	2.455

APPENDIX C
LIST OF PUBLICATIONS

Ployprapai Mongkolsamai and Tawatchai Charinpanitkul, ‒Synthesis of magnetic carbon nanoparticles by using pyrolysis of ethanol and ferrocene" Poster Presentation on the 1st Joint Conference on Renewable Energy and Nanotechnology (JCREN), Imperial Queen's Park Hotel, Bangkok, Thailand, November 19-20,2012

Ployprapai Mongkolsamai, Kanokwan Sowichai, Kenji Shiratai, Kornrat Kerdnawee, and Tawatchai Charinpanitkul, ‒Removal of antibiotics in wastewater using magnetic carbon nanoparticles" Oral Presentation on the th Asia-Oceania Top University League on Engineering (AOTULE), Faculty of Engineering, University of Malaya, Malaysia, November 24-25, 2012

Ployprapai Mongkolsamai, Kenji Shiratai, Kornrat Kerdnawee and Tawatchai Charinpanitkul, ‒Synthesis of magnetic carbon nanostructures from ethanol using co-pyrolysis with ferrocene" Poster Presentation on 10th Biomass-Asia Workshop "Biomass Refinery to Community and Industrial Applications", Centara Grand at Central World Hotel, Bangkok, Thailand, August 5 - 6, 2013

VITA

Miss Ployprapai Mongkolsamai was born in April 27, 1988, in Bangkok, Thailand. She completed her high-school education at Santa Cruz Convent School. She received a graduated Bachelor Degree of Science with the department of Chemical Technology from Chulalongkorn University. After that, she decided to study in Master degree in Center of Excellence in Particle Technology at Department of Chemical Engineering, Faculty of Engineering, Chulalongkorn University with the thesis entitled ―Treatment of wastewater contaminated with antibiotics using magnetic carbon nanoparticles".